

Exploiting Intraday Decompositions in Realized Volatility Forecasting: A Forecast Reconciliation Approach

Massimiliano Caporin

Department of Statistical Sciences, University of Padova

Email: massimiliano.caporin@unipd.it

Tommaso Di Fonzo

Department of Statistical Sciences, University of Padova

Email: tommaso.difonzo@unipd.it

Daniele Girolimetto

Department of Statistical Sciences, University of Padova

Email: daniele.girolimetto@phd.unipd.it

June 6, 2023

Abstract

We address the construction of Realized Variance (RV) forecasts by exploiting the hierarchical structure implicit in available decompositions of RV . By using data referred to the Dow Jones Industrial Average Index and to its constituents we show that exploiting the informative content of hierarchies improves the forecast accuracy. Forecasting performance is evaluated out-of-sample based on the empirical MSE and $QLIKE$ criteria as well as using the Model Confidence Set approach.

Keywords: Realized Volatility, Good and Bad Volatility, HERO, Hierarchical Forecasting, Forecast reconciliation.

JEL: C10, C13, C32, C33, C55, C58

1 Introduction

Volatility forecasting has attracted a relevant amount of interest in the financial econometrics literature since the seminal contribution of Engle (1982). The reasons are well-known and ground on the importance of volatility in several areas, from risk management to asset allocation, from hedging to pricing. In the last two decades the interest has shifted from conditional variance models to the modeling and forecasting of Realized Variances, RV (Andersen et al., 2001a,b, 2003). In this case, starting from the work of Corsi (2009), based on the introduction of a simple specification capable of capturing the strong serial correlation of RV sequences, several additional specifications have been introduced. These include models including price jumps in the variance dynamic (Andersen et al., 2007a), controlling for residual heteroskedasticity (Corsi and Renó, 2012), dealing with measurement errors (Bollerslev et al., 2016), disentangling the role of positive and negative returns (Patton and Sheppard, 2015), and considering a quantile-based intraday decomposition of RV (Bollerslev et al., 2022). From a pure forecasting perspective, despite all models might provide statistical and/or economic advantages compared to simpler specifications, there is no clear evidence that a model clearly superior to all competitors exists (Caporin, 2022).

A few contributions share a common feature from the modeling perspective: to predict the RV they extract information from a decomposition of lagged RV . This holds, in particular, when separating the continuous and discontinuous variance components, as in Andersen et al. (2007a), or when ‘Good and Bad’ volatilities are used, as in Patton and Sheppard (2015), or when the two approaches are combined (Caporin, 2022), or finally when a more flexible decomposition according to conditional and time-varying intraday returns quantiles is considered (Bollerslev et al., 2022). In all of these cases, the decomposition provides what is known as a *hierarchy* in the hierarchical forecasting literature (Hyndman et al., 2011), that is a structure in which an aggregate series (e.g., daily RV) can be seen at the top over its constituents series (e.g., intraday RV decompositions).

Therefore, when dealing with intraday data, sometimes the observed returns may be

grouped based on some criterion of similarity, such as the sign, or the occurrence in portions of the intraday returns density support. This decomposition may be employed in forecasting the daily RV , through segment-level forecasting within each segment. Challenges associated with successfully applying intraday decompositions include how to create segments and how to combine the segment-level RV forecasts to recover a daily RV forecast. The current paper proposes a method to exploit existing and to create new decompositions of the daily RV based on high-frequency intraday data, create segment-level forecasts, and then combine these forecasts to improve the daily RV forecasts. We present a combined-aggregative forecasting method for daily RV that allows to obtain a global prognosis by summing up/combining the forecasts of the compounding individual components. We detail a bottom-up (indirect) and a regression-based forecast reconciliation (Hyndman et al., 2011, Wickramasuriya et al., 2019) approach, and study their forecasting performance *vis-à-vis* the daily direct RV forecasts produced by the classic HAR model (Corsi, 2009), and two variants that take into account intraday RV decompositions (Patton and Sheppard, 2015, Bollerslev et al., 2022). At this end, we have devised a forecasting experiment to evaluate the new proposed forecasting approaches on the high-frequency data of a few assets. The proposed method utilizes standard forecasting tools, but applies them in a unique combination that results in a higher level of daily RV forecast accuracy than other traditional methods.

A common technique used to forecast an aggregate involve bottom-up method. This procedure starts from forecasting all bottom-level components and then obtaining the top-level forecast by simply summing these bottom-level forecasts. By contrast, the direct approach simply produces forecasts at the top level. Nevertheless, realized volatility in different segments of the day usually have quite different patterns, hence the trivial approach of only forecasting the bottom-level series is unlikely to provide very accurate forecasts for the top-level series. In addition, the different behaviour of RV at different time periods, suggests to group the observed volatility according to different time intervals. This may be consid-

ered either alone or in conjunction with other grouping schemes related to the nature of the volatility itself (i.e., ‘Good & Bad’ volatility, Patton and Sheppard, 2015). This gives rise to a hierarchical/grouped time series, where daily RV may be seen as the top-level series of a hierarchy, whose bottom level consists of the components obtained by crossing time periods and volatility decompositions. In this case, besides bottom-up, another (hopefully) more accurate method for hierarchical forecasting is to independently generate RV forecasts at all levels of the hierarchy. The advantage of independently generating the forecasts at each level is that each level can customize its forecasting model according to the varying characteristic of the RV at its own level. Thus, such approach could provide more accurate top-level forecasts than traditional direct or bottom-up approaches. However, these independently-made forecasts have the undesirable consequence that the lower-level forecasts cannot add up exactly to the higher-level forecasts. Thus, it is necessary to carry out some adjustments to ensure that hierarchical forecasts meet the constraints introduced by the hierarchical structure in the same way as their measurement data, i.e., in each day the sum of the lower-level intraday RV components forecasts should be equal to the higher-level daily RV forecast.

The methodology we put forward comprises two steps:

1. *Independent forecasting of daily RV and its components*, generating the so called ‘base forecasts’. For the daily RV series and for all its intraday components from a specific decomposition we issue a forecast as accurate as possible, using three different HAR-based forecasting models proposed in the literature. In general, the base forecasts are not coherent with the additive decomposition law linking the observed daily RV s to its observed intraday components.
2. *Aggregation post-process*. We then combine these forecasting results to forecast the h -day-ahead RV , where $h \geq 1$ is the forecast horizon. In this paper, we consider a postprocess aggregation method suggested in the vast literature on regression-based cross-sectional forecast reconciliation (Hyndman et al., 2011, Wickramasuriya et al., 2019).

We compare the accuracy of the aggregate (direct) forecasting with the disaggregate (indirect) bottom-up and the regression-based forecast-reconciliation approach for the daily RV of the Dow Jones Industrial Average index and 26 of its constituents assets. Most of the existing studies on forecasting daily RV did not consider possible hierarchical structures deriving from intraday decompositions of the RV , and often missed the coherent relationships between individual components. An exception is Sohn and Lim (2007), who evaluated aggregate *vs.* disaggregate forecasting of 30 simulated coherent components of the DJIA index based on the AR(2)-GARCH(1,1) model. However, the results of this experiment were quite inconclusive, as it was found that the accuracy of the indirect forecasting method varied depending on the correlation degree of the coherent components. Instead, and contrary to Sévy (2014), our results indicate that considering the various components of the realized variance do represent a significant improvement in an out-of-sample forecast evaluation framework.

The paper proceeds as follows. The forecast reconciliation methodology is reviewed in Section 2. Section 3 briefly describes the volatility modeling and introduces the hierarchies. The empirical setup of the out-of-sample forecasting experiment is described in Section 4, and Section 5 shows the results. A robustness analysis is performed in Section 6. Finally, conclusive remarks and indications for future developments are proposed in Section 7.

2 Forecast reconciliation: a recap

Forecast reconciliation is a post-forecasting process aimed to improve the quality of the *base* forecasts for a system of hierarchical/grouped, and more generally linearly constrained, time series by exploiting the constraints that the series in the system must fulfil, whereas in general the base forecasts do not; see, among others, Hyndman et al. (2011) and Girolimetto and Di Fonzo (2023b). Following Panagiotelis et al. (2021), a linearly constrained time series \mathbf{y}_t is defined as a n -dimensional time series such that all observed values $\mathbf{y}_1, \dots, \mathbf{y}_T$ and all future values $\mathbf{y}_{T+1}, \mathbf{y}_{T+2}, \dots$ lie in the coherent linear subspace $\mathcal{S} \subset \mathbb{R}^n$, that is: $\mathbf{y}_t \in \mathcal{S}, \forall t$.

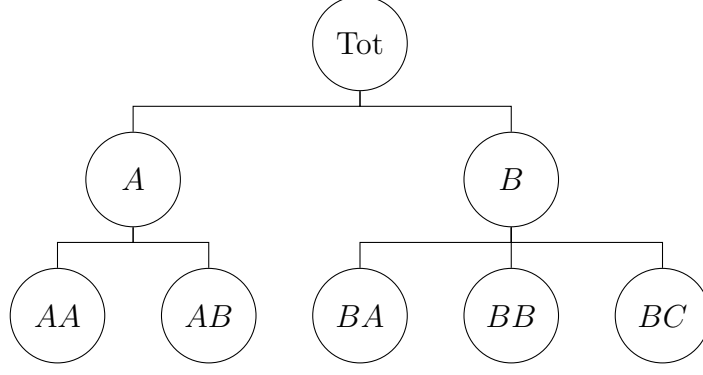


Figure 1: A simple three-level hierarchical structure.

In many cases, the linear constraints can be represented as a hierarchy, where the time series are linked through summation constraints. Figure 1 shows an example of a hierarchical time series with eight variables and three levels: the top-variable at level 0, two variables (A and B) at level 1, and five variables at level 2 (AA, AB, BA, BB, BB, BC). The 3 aggregated upper time series are linked to the bottom-level variables through summation:

$$\begin{aligned}
 y_{Tot,t} &= y_{A,t} + y_{B,t} \\
 y_{A,t} &= y_{AA,t} + y_{AB,t} \\
 y_{B,t} &= y_{BA,t} + y_{BB,t} + y_{BC,t}
 \end{aligned}
 \quad \forall t = 1, \dots, T.$$

The bottom-level series can be thought of as building blocks that cannot be obtained as sum of other series in the hierarchy, while all the series at upper levels can be expressed by appropriately summing part or all of them. In details, let \mathbf{b}_t and \mathbf{a}_t be the vectors of bottom level and upper level time series at time t , respectively. For example, $\mathbf{b}_t = [y_{AA,t} \ y_{AB,t} \ y_{BA,t} \ y_{BA,t} \ y_{BA,t}]'$, $\mathbf{a}_t = [y_{Tot,t} \ y_{A,t} \ y_{B,t}]'$. Denoting by \mathbf{y}_t the vector $\mathbf{y}_t = [\mathbf{a}_t' \ \mathbf{b}_t']'$, the relationships linking bottom and upper time series can be equivalently expressed as:

$$\mathbf{a}_t = \mathbf{A}\mathbf{b}_t, \quad \mathbf{y}_t = \mathbf{S}\mathbf{b}_t, \quad \mathbf{C}\mathbf{y}_t = \mathbf{0}_{(n_a \times 1)}, \quad t = 1, \dots, T. \quad (1)$$

where \mathbf{A} is the $(n_a \times n_b)$ aggregation matrix, $\mathbf{S} = \begin{bmatrix} \mathbf{A} \\ \mathbf{I}_{n_b} \end{bmatrix}$ is the $(n \times n_b)$ structural matrix and $\mathbf{C} = [\mathbf{I}_{n_a} \quad -\mathbf{A}]$ is the $(n_a \times n)$ zero constraints matrix. We call *structural representation*

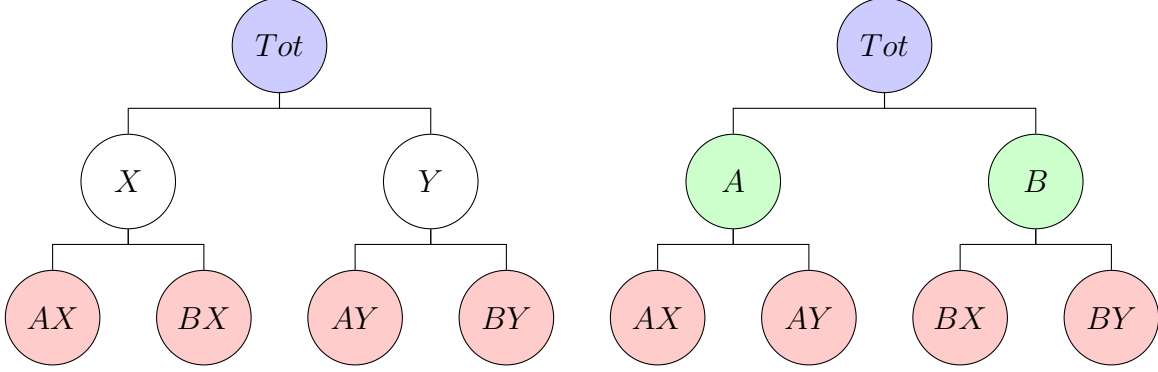


Figure 2: *A simple grouped structure.*

of series \mathbf{y}_t the formulation $\mathbf{y}_t = \mathbf{S}\mathbf{b}_t$, $t = 1, \dots, T$, and *zero-constrained representation* of series \mathbf{y}_t the equivalent expression $\mathbf{C}\mathbf{y}_t = \mathbf{0}$, $t = 1, \dots, T$.

A linearly constrained time series formed by two or more hierarchical time series sharing the same top level series, and the same bottom level series, is called *grouped time series* (Hyndman et al., 2011). An example is shown in Figure 2, where the Total variable can be described as two different hierarchies with intermediate variables (X, Y) and (A, B) , respectively, which share the same four bottom-level variables (AX, BX, AY, BY) . Provided matrix \mathbf{A} is appropriately designed, the definitions of matrices \mathbf{S} and \mathbf{C} remain unchanged.

Now, suppose we have the $(n \times 1)$ vector $\hat{\mathbf{y}}_h$ of unbiased base forecasts for the n variables of the linearly constrained series \mathbf{y}_t for the forecast horizon h . If the base forecasts have been independently computed, generally, they do not fulfil the cross-sectional aggregation constraints, that is, $\mathbf{C}\hat{\mathbf{y}}_h \neq \mathbf{0}_{(n \times 1)}$. The aim of forecast reconciliation is to adjust the base forecast $\hat{\mathbf{y}}_h$ by using a mapping $\psi : \mathbb{R}^n \rightarrow \mathcal{S}$ to obtain the reconciled forecast vector $\tilde{\mathbf{y}}_h = \psi(\hat{\mathbf{y}}_h)$, where $\tilde{\mathbf{y}}_h \in \mathcal{S}$. The mapping ψ can be defined as a projection onto \mathcal{S} (van Erven and Cugliari, 2015, Panagiotelis et al., 2021, Di Fonzo and Girolimetto, 2023):

$$\tilde{\mathbf{y}}_h = \mathbf{M}\hat{\mathbf{y}}_h, \quad (2)$$

where $\mathbf{M} = \mathbf{I}_n - \mathbf{W}\mathbf{C}'(\mathbf{C}\mathbf{W}\mathbf{C}')^{-1}\mathbf{C}$, with \mathbf{W} error covariance matrix of the base forecasts $\hat{\mathbf{y}}$. Another way to obtain the reconciled forecasts is through the structural approach

proposed by Hyndman et al. (2011), such that

$$\tilde{\mathbf{y}}_h = \mathbf{S}\mathbf{G}\hat{\mathbf{y}}_h, \quad (3)$$

where $\mathbf{G} = (\mathbf{S}'\mathbf{W}^{-1}\mathbf{S})^{-1}\mathbf{S}'\mathbf{W}^{-1}$, and it can be shown that $\mathbf{M} = \mathbf{S}\mathbf{G}$ (Wickramasuriya et al., 2019). Several alternatives have been provided in the literature to approximate the covariance matrix \mathbf{W} (Hyndman et al., 2011, 2016; Wickramasuriya et al., 2019). In this work, we will consider the state of the art shrinkage covariance matrix approximation proposed by Wickramasuriya et al. (2019),

$$\mathbf{W} = \hat{\lambda}\widehat{\mathbf{W}}_D + (1 - \hat{\lambda})\widehat{\mathbf{W}}_1,$$

where $\widehat{\mathbf{W}}_1 = \frac{1}{T} \sum_{t=1}^T \hat{\mathbf{e}}_t \hat{\mathbf{e}}_t'$ is the covariance matrix of the one-step ahead in-sample forecast errors ($\hat{\mathbf{e}}_t = \mathbf{y}_t - \hat{\mathbf{y}}_t$, $t = 1, \dots, T$), $\widehat{\mathbf{W}}_D = \mathbf{I}_n \odot \widehat{\mathbf{W}}_1$, and \odot denotes the Hadamard product.

In the next section, after briefly reviewing the estimation of RV , we link the hierarchical forecasting literature to the RV modeling one.

3 RV modeling: a hierarchical perspective

The measurement of daily RV builds on the availability of data at a frequency higher than the day. If we denote by $t = 1, \dots, T$, the daily time index, and by $i = 1, 2, \dots, N$, the intraday time index, the prices of a financial instrument observed in high frequency are denoted by $P_{i,t}$. From the prices we move to log-returns $r_{i,t}$ and to the estimation of RV in a given day as follows:

$$RV_t = \sum_{i=1}^N [\log(P_{i,t}) - \log(P_{i-1,t})]^2 = \sum_{i=1}^N r_{i,t}^2, \quad (4)$$

where prices at the intraday level are assumed to be observed on an equally spaced time grid (e.g., every minute), and for $i = 1$ the lagged price corresponds to the opening price of the day, thus excluding the overnight return from the evaluation. The financial econo-

metrics literature has extensively discussed the issue of estimation of RV in the presence of microstructure noise and of price jumps; see, among many others, Aït-Sahalia and Jacod (2014) and therein cited references. In this work, we refer to the simplest approach reported above. Moreover, as our final purpose is to adopt hierarchical forecast reconciliation approaches starting from the forecast of bottom time series, we do not consider the decomposition of RV into its continuous and discontinuous component, since it is known that the discontinuous component is not predictable by means of relatively simple linear models; among the possible approaches, see Andersen et al. (2011) and Aït-Sahalia et al. (2015).

As mentioned in the introduction, several authors have focused on decompositions of RV . The most known example is given by the use of signed variations, as in Patton and Sheppard (2015), such that $RV_t = SV_t^+ + SV_t^-$, with

$$SV_t^+ = \sum_{i=1}^N r_{i,t}^2 I(r_{i,t} \geq 0) \quad \text{and} \quad SV_t^- = \sum_{i=1}^N r_{i,t}^2 I(r_{i,t} < 0)$$

where $I(a)$ is an indicator function taking unit value when condition a is true and zero otherwise. The signed variations are also known as *Semi-Variations* (Barndorff-Nielsen et al., 2010), or as *Good* (SV_t^+) and *Bad* (SV_t^-) volatility, respectively, and separate the contribution to RV coming from upside and downside price movements.

More recently, Bollerslev et al. (2022) introduced a quantile-based decomposition, generalizing the signed variation approach, $RV_t = \sum_{l=1}^p PV_t^{(l)}$, with

$$PV_t^{(l)} = \sum_{i=1}^N r_{i,t}^2 I(\mathcal{Q}_{r,t}(\alpha_{l-1}) < r_{i,t} \leq \mathcal{Q}_{r,t}(\alpha_l)),$$

where $\mathcal{Q}_{r,t}(\tau) = \sqrt{N^{-1}RV_t} \mathcal{Q}_{z,t}(\tau)$, $z^{i,t} = \frac{r_{i,t}}{\sqrt{N^{-1}RV_t}}$ is the standardized intraday return, $\mathcal{Q}_{z,t}(\tau)$ is the empirical τ -quantile of the intraday standardized returns distribution in day t , $\mathcal{Q}_{r,t}(\alpha_0) = -\infty$ and $\mathcal{Q}_{r,t}(\alpha_p) = +\infty$, and $0 < \alpha_1 < \dots < \alpha_{p-1} < 1$ is a sequence of probabilities. The $PV_t^{(l)}$ components, also called *Partial Variances*, allow separating the

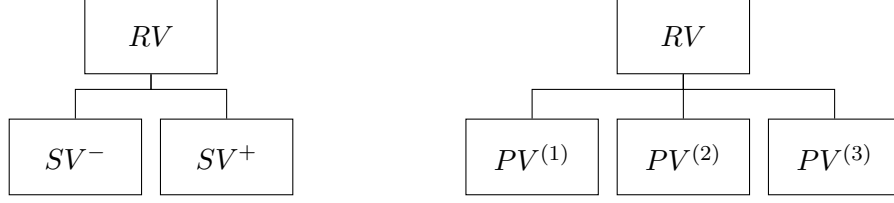


Figure 3: Hierarchical representations of the Bad and Good (left, Patton and Sheppard, 2015) and $PV(3)$ (right, Bollerslev, 2022) decompositions of daily RV .

contribution to RV coming from intraday returns according to both their sign and size.

The concept of hierarchical time series in the framework of forecasting daily RV using its intraday decompositions may be illustrated by considering the two simple hierarchies deriving from the intraday RV decompositions reported above, i.e. Patton and Sheppard (2015) and Bollerslev (2022), the last in the simple case with $p = 2$. Figure 3 provides a graphical representation of the two hierarchies.

To illustrate the advantage and flexibility of forecast reconciliation approaches in the RV context, we provide a more general form of temporal and threshold-based decomposition of daily RV . The use of quantiles computed from intraday returns is, in practice, a special case of a grouping of returns according to pre-defined, possibly time-varying thresholds, with general representation given by:

$$z_{l,t} = \sum_{t=1}^N r_{i,t}^2 I(c_{t,l-1} < r_{i,t} \leq c_{t,l}), \quad l = 1, \dots, p, \quad (5)$$

where $c_{t,0} = -\infty$ and $c_{t,p} = +\infty$.

Differently, by exploiting the availability of information distributed over a range of minutes within a given day, we might group the intraday returns according to a temporal scheme

$$w_{k,t} = \sum_{i=m(k-1)+1}^{mk} r_{i,t}^2, \quad k = 1, \dots, \frac{N}{m}, \quad (6)$$

which is equivalent to

$$w_{k,t} = \sum_{t=1}^N r_{i,t}^2 I(m(k-1) < i \leq mk), \quad k = 1, \dots, \frac{N}{m}. \quad (7)$$

Temporal decomposition	Semi-Variances	
	$r_{t,i} < 0$ SV^-	$r_{t,i} \geq 0$ SV^+
T1: minutes 1-78	T1SV ⁻	T1SV ⁺
T2: minutes 79-156	T2SV ⁻	T2SV ⁺
T3: minutes 157-234	T3SV ⁻	T3SV ⁺
T4: minutes 235-312	T4SV ⁻	T4SV ⁺
T5: minutes 313-390	T5SV ⁻	T5SV ⁺

Table 1: *The ten bottom variables from the time-by-‘Good & Bad’ volatility decompositions.*

The threshold- and time-based decompositions might be combined giving rise to the most disaggregated (bottom level) time series, defined as

$$x_{l,k,t} = \sum_{t=1}^N r_{i,t}^2 I[(c_{t,l-1} < r_{i,t} \leq c_{t,l}) \cap (m(k-1) < i \leq mk)], \quad \begin{matrix} l = 1, \dots, p \\ k = 1, \dots, \frac{N}{m} \end{matrix}, \quad (8)$$

or

$$x_{l,k,t} = \sum_{i=m(k-1)+1}^{mk} r_{i,t}^2 I(c_{t,l-1} < r_{i,t} \leq c_{t,l}), \quad \begin{matrix} l = 1, \dots, p \\ k = 1, \dots, \frac{N}{m} \end{matrix}, \quad (9)$$

For example, assuming a day consisting of 6.5 hours, with data available at the 1-minute frequency ($N = 390$), setting $p = 3$ and $m = 78$, we have the following decompositions of RV :

RV	w_1	w_2	w_3	w_4	w_5
z_1	$x_{1,1}$	$x_{1,2}$	$x_{1,3}$	$x_{1,4}$	$x_{1,5}$
z_2	$x_{2,1}$	$x_{2,2}$	$x_{2,3}$	$x_{2,4}$	$x_{2,5}$
z_3	$x_{3,1}$	$x_{3,2}$	$x_{3,3}$	$x_{3,4}$	$x_{3,5}$

where the threshold-based $z_l = \sum_{k=1}^5 x_{l,k}$, $l = 1, \dots, 3$, and temporal-based $w_k = \sum_{l=1}^3 x_{l,k}$, $k = 1, \dots, 5$, decompositions represent the marginals of a combined and richer decomposition.

We also note that $RV = \sum_{k=1}^5 w_k = \sum_{l=1}^3 z_l = \sum_{l=1}^3 \sum_{k=1}^5 x_{l,k}$.

In the following empirical analyses, we will make use of the hierarchies/groupings generated by crossing a temporal decomposition in five non-overlapping intervals of 78 minutes each, with either (ii) the dichotomous intraday decomposition in ‘Good and Bad’ volatility

Temporal decomposition	Quantile-based decomposition		
	$r_{t,i} \leq Q(10\%)$ $PV^{(1)}$	$Q(10\%) < r_{t,i} \leq Q(75\%)$ $PV^{(2)}$	$r_{t,i} > Q(75\%)$ $PV^{(3)}$
T1: minutes 1-78	T1PV ⁽¹⁾	T1PV ⁽²⁾	T1PV ⁽³⁾
T2: minutes 79-156	T2PV ⁽¹⁾	T2PV ⁽²⁾	T2PV ⁽³⁾
T3: minutes 157-234	T3PV ⁽¹⁾	T3PV ⁽²⁾	T3PV ⁽³⁾
T4: minutes 235-312	T4PV ⁽¹⁾	T4PV ⁽²⁾	T4PV ⁽³⁾
T5: minutes 313-390	T5PV ⁽¹⁾	T5PV ⁽²⁾	T5PV ⁽³⁾

Table 2: *The fifteen bottom variables from the time-by-quantile daily decompositions according to $PV(3)$.*

(Patton and Sheppard, 2015, see Table 1 and Appendices 2 and 3), or (ii) a quantile-based decomposition with $p = 3$, where, on the basis of the results found by Bollerslev et al. (2022), the quantile thresholds are exogenously fixed at 10% and 75%, respectively (see Table 2 and Appendices 2 and 3). The Appendices report the graphical and structural representations of the hierarchies.

4 The empirical setup

4.1 Data description and analysis

We evaluate the impact of forecast reconciliation in forecasting daily RV of individual stocks included in the Dow Jones Industrial Average (DJIA) index, from the beginning of January 2003 to the end of June 2022. We use price data at the 1-minute frequency, adjusted for splits and dividends. We consider prices recorded from 9:00 AM to 3:59 PM (time identifies the start of each intraday interval), obtaining 390 observations per day. Our dataset includes 4,908 full days excluding weekends, holidays and closed market days. The data have been recovered from Kibot.com.¹ We consider the 26 stocks whose data are available to us for the entire sample, denoted by the following tickers:² AAPL, AMGN, AXP, BA, CAT, CSCO, CVX, DIS, GS, HD, HON, IBM, INTC, JNJ, JPM, KO, MCD, MMM, MRK, MSFT, NKE,

¹The quality of data from Kibot.com is comparable to that of NYSE TAQ data. A comparison on a selected equity is available from authors upon request.

²Appendix A1 contains a summary description of the data used in the forecasting experiment.

PG, UNH, VZ, WBA, and WMT. The use of DJIA constituents is in line with the choice made by Bollerslev et al. (2022) and allows dealing with the possible presence of large amount of zeros at the intraday level. In fact, for those highly liquid stocks, the presence of zeros is extremely limited.

Starting from the 1-minute data, we estimate the daily RV , and the decompositions (hierarchies) we previously mentioned. First of all, we decompose the RV into the Good and the Bad components, following Patton and Sheppard (2015); this gives a hierarchy with two bottom series. Second, following Bollerslev et al. (2022), we decompose RV into the Partial Variances $PV^{(g)}$. Differently from the authors, we do not optimally select the quantiles used for the decomposition, nor we allow for a time-change in the quantile. On the contrary, building on the evidence in Bollerslev et al. (2022), and in particular on the values in Table 2 of their paper, we select the $PV(3)$ decomposition with fixed quantiles set at the 10% and 75% thresholds. This gives a hierarchy with three bottom series, and allows us to simplify the treatment and the following analyses. Third, we apply both the Good and Bad and $PV(3)$ decompositions on sub-samples of the day. We first divide the entire day in 5 sub-intervals of length equal to 78 observations (minutes), and in each sub-sample we apply either the Good and Bad or the $PV(3)$ decompositions. We note that this gives, overall, 10 bottom series in the former case, and 15 in the latter. In addition, we do have two possible intermediate aggregations, by temporal sub-sample, or by volatility (either SV or $PV(3)$) components. The hierarchies/groupings in this case are thus much richer than if only volatility-based decompositions are used (see the Appendix for additional details and results).

4.2 Base forecasts: direct forecasts from benchmark models and intraday components' forecasts

In the past years, the subject of the comparison of the forecast accuracy of aggregating disaggregate forecasts versus forecasts based on aggregated data has received attention in

different fields, as macro-economic (Marcellino et al., 2003, Frale et al., 2011, Poncela and García-Ferrer, 2014, Grassi et al., 2015), demand (Petropoulos et al., 2014, Mircetic et al., 2022), and energy (Silva et al., 2018, Wang et al., 2021) forecasting. However, as far as we know, a detailed comparison of direct, indirect (bottom-up) and combination (forecast reconciliation) procedures for daily RV forecasting has not been provided yet.

At this end, we conduct an out-of-sample forecasting experiment where we compare direct daily- RV forecasts with three reference models proposed, respectively, by Corsi (2009), Patton and Sheppard (2015), and Bollerslev et al. (2022), two indirect forecasts obtained through simple bottom-up of the HAR forecasts of either semi-variances (Barndorff-Nielsen et al., 2010) or partial-variances (Bollerslev et al., 2022) components, and finally the daily forecasts of RV obtained through forecast reconciliation of both the aggregate (daily RV) and disaggregate (corresponding components of the daily RV) forecasts.

The modeling strategy we adopt for each of the bottom and top time series, and that we will use to produce direct and base forecasts, is very simple. As our purpose is to introduce the use of forecast reconciliation tools in the prediction of RV , and not to identify the best forecasting univariate model, we fit on all (possibly disaggregate) time series the HAR model of Corsi (2009). Let x_t be a generic time series, that is, either RV_t or one of the bottom series according to one of the hierarchies previously introduced. We model x_t as follows:

$$x_t = \beta_0 + \beta_D x_{t-1} + \beta_W x_{t-1:t-5} + \beta_M x_{t-1:t-22} + \varepsilon_t, \quad (10)$$

where $x_{t-1:t-m} = \frac{1}{m} \sum_{j=1}^m x_{t-j}$ and ε_t is an innovation term. Parameters refer to the intercept (β_0) and to the daily, weekly and monthly effects (β_D , β_W , and β_M , respectively). Parameter estimation is based on least squares and we adopt robust standard errors to be coherent with the *volatility-of-volatility* effect (Corsi et al., 2008). Further, we do not consider the modeling of logarithms of RV_t leaving to future researches the generalization of our approach along this line.³

³We stress the use of the logarithmic transformation of RV sensibly impacts on the aggregation constraints, with the need of moving toward probabilistic hierarchical forecasting approaches.

Models for daily RV (direct and base forecasts)

HAR: Heterogeneous AutoRegressive model

$$RV_t = \alpha_0 + \alpha_D RV_{t-1} + \alpha_W RV_{t-1:t-5} + \alpha_M RV_{t-1:t-22} + \varepsilon_t^{HAR}$$

SV: Semi-Variates Heterogeneous AutoRegressive model

$$RV_t = \beta_0 + \beta_D^+ SV_{t-1}^+ + \beta_D^- SV_{t-1}^- + \beta_W RV_{t-1:t-5} + \beta_M RV_{t-1:t-22} + \varepsilon_t^{SHAR}$$

PV(3): Partial-Variates Heterogeneous AutoRegressive model

$$RV_t = \gamma_0 + \sum_{l=1}^3 \gamma_D^{(j)} PV_{t-1}^{(l)} + \gamma_W RV_{t-1:t-5} + \gamma_M RV_{t-1:t-22} + \varepsilon_t^{PV_3}$$

HAR-type models for intraday RV decompositions (base forecasts)

Semi-variances decomposition

$$SV_t^+ = \delta_0^+ + \delta_D^+ SV_{t-1}^+ + \delta_W^+ SV_{t-1:t-5}^+ + \delta_M^+ SV_{t-1:t-22}^+ + \varepsilon_t^{SHAR^+}$$

$$SV_t^- = \delta_0^- + \delta_D^- SV_{t-1}^- + \delta_W^- SV_{t-1:t-5}^- + \delta_M^- SV_{t-1:t-22}^- + \varepsilon_t^{SHAR^-}$$

Partial-variances decomposition ($l = 1, 2, 3$)

$$PV_t^{(l)} = \theta_0^{(l)} + \theta_D^{(l)} PV_{t-1}^{(1)} + \theta_W^{(l)} PV_{t-1:t-5}^{(l)} + \theta_M^{(l)} PV_{t-1:t-22}^{(l)} + \varepsilon_t^{PV^{(l)}}$$

Time-variances decomposition ($j = 1, 2, 3, 4, 5$)

$$T_{j,t} = \eta_0^j + \eta_1^j T_{j,t-1} + \eta_2^j T_{j,t-1:t-5} + \eta_3^j T_{j,t-1:t-22} + \varepsilon_t^{T(j)}$$

Time- and semi-variances decomposition ($j = 1, 2, 3, 4, 5$)

$$T_j SV_t^- = \lambda_0^{j-} + \lambda_1^{j-} T_j SV_{t-1}^- + \lambda_2^{j-} T_j SV_{t-1:t-5}^- + \lambda_3^{j-} T_j SV_{t-1:t-22}^- + \varepsilon_t^{T(j)SV^-}$$

$$T_j SV_t^+ = \lambda_0^{j+} + \lambda_1^{j+} T_j SV_{t-1}^+ + \lambda_2^{j+} T_j SV_{t-1:t-5}^+ + \lambda_3^{j+} T_j SV_{t-1:t-22}^+ + \varepsilon_t^{T(j)SV^+}$$

Time- and partial-variances decomposition ($j = 1, 2, 3, 4, 5, l = 1, 2, 3$)

$$T_j PV_t^{(l)} = \eta_0^{j,l} + \eta_1^{j,l} T_j PV_{t-1}^{(l)} + \eta_2^{j,l} T_j PV_{t-1:t-5}^{(l)} + \eta_3^{j,l} T_j PV_{t-1:t-22}^{(l)} + \varepsilon_t^{T(j)PV^{(l)}}$$

Table 3: Models used to produce daily (direct and base) RV forecasts, and base forecasts of intraday RV decompositions according to either semi-variances or partial-variances, alone or with time-groupings of non-overlapping 78 consecutive minutes intervals.

For the top-level variable (i.e., daily RV) forecasts, we consider other two reference models proposed by Patton and Sheppard (2015) and Bollerslev et al. (2022) to account for, respectively, Good and Bad volatility and Partial Variances. In this last case, for simplicity, we consider an *ex-ante* choice of the two quantiles defining the three partial-variances decomposition (see Table 3).

We obtain daily forecasts for the time series of the daily semi-variances according to the

‘Good & Bad’ (Barndorff-Nielsen et al., 2010, Patton and Sheppard, 2015) and to the $PV(3)$ decompositions (Bollerslev et al., 2022), then we apply a simple bottom-up procedure to compute indirect forecasts of the daily RV . Finally, the forecasts obtained in the two previous steps are combined through the forecast reconciliation approach proposed by Wickramasuriya et al. (2019) (see also Hyndman et al., 2011), which is a regression-based forecast combination approach exploiting the simple hierarchical structure of the two considered decomposition settings. The competing forecasting approaches, and the corresponding acronyms, are the following ones (reported for a one-period forecast horizon):

Direct forecasting procedures

- HAR : \widehat{RV}_{t+1}^{HAR} (Corsi, 2009);
- SV : \widehat{RV}_{t+1}^{SV} (Patton and Sheppard, 2015);
- $PV(3)$: $\widehat{RV}_{t+1}^{PV(3)}$ (Bollerslev et al., 2022);

Indirect forecasting procedures (bottom-up)

- SV_{bu} : $\widehat{RV}_{t+1}^{SV_{bu}} = \widehat{SV}_{t+1}^+ + \widehat{SV}_{t+1}^-$;
- $PV(3)_{bu}$: $\widehat{RV}_{t+1}^{PV(3)_{bu}} = \widehat{PV}_{t+1}^{(1)} + \widehat{PV}_{t+1}^{(2)} + \widehat{PV}_{t+1}^{(3)}$;

Forecast reconciliation procedures

- SV_{shr} : $\widehat{RV}_{t+1}^{SV_{shr}} = f(\widehat{RV}_{t+1}^{SV}, \widehat{SV}_{t+1}^+, \widehat{SV}_{t+1}^-)$;
- $PV(3)_{shr}$: $\widehat{RV}_{t+1}^{PV(3)_{shr}} = f(\widehat{RV}_{t+1}^{PV_3}, \widehat{PV}_{t+1}^{(1)}, \widehat{PV}_{t+1}^{(2)}, \widehat{PV}_{t+1}^{(3)})$.

We will always use the above-reported acronyms independently from the forecast horizon we consider. Coherently with the common practice, see, for instance, (Patton and Sheppard, 2015), when the forecast horizon differs from 1 and become h , we set the dependent variable of our model to the h –period average cumulative value.⁴

⁴In this case, equation 10 becomes $x_{t+h-1:t} = \beta_0 + \beta_D x_{t-1} + \beta_W x_{t-1:t-5} + \beta_M x_{t-1:t-22} + \varepsilon_t$, with $x_{t+h-1:t}$ being the average of x_{t+i} for $i = 0, 1, \dots, h-1$.

4.3 Out-of-sample forecast evaluation

We perform a fixed length rolling window forecasting experiment on the DJIA series and 26 individual stocks previously mentioned. The first training set spans the period January 2, 2003 - December 29, 2006 (1,007 days). From each training set three direct multistep forecasts for, respectively, one-, five- and twenty-two-steps (day) ahead are computed, and this is done for all the time series components of the various hierarchies defined by the time-and/or-quantile-based RV_t intraday decompositions.

The base forecasts of the top-level series in each hierarchy (RV_t) are obtained according to the *HAR*, *SV* and *PV*(3) models, respectively. The base forecasts of either the semi- or partial-variances series forming each hierarchy are obtained using appropriately adapted *HAR* models. The base forecasts are then reconciled through the MinT-shr approach (Wickramasuriya et al., 2019) using the R package *FoReco* (Girolimetto and Di Fonzo, 2023a). The point forecast accuracy of daily RV_t is evaluated using the Mean Square Error (*MSE*), and the *QLIKE* index (Patton, 2011b):⁵

$$\begin{aligned} MSE &= \frac{1}{|\mathcal{S}|} \sum_{t=1}^{|\mathcal{S}|} \left(\widehat{RV}_t - RV_t \right)^2 \\ QLIKE &= \frac{1}{|\mathcal{S}|} \sum_{t=1}^{|\mathcal{S}|} \left(\frac{RV_t}{\widehat{RV}_t} - \frac{\log RV_t}{\log \widehat{RV}_t} - 1 \right), \end{aligned} \quad (11)$$

where \widehat{RV}_t and $|\mathcal{S}|$ denote the one-step-ahead forecast and the number of days in the test set, respectively. Both *MSE* and *QLIKE* belong to the family of loss functions of Patton (2011b), that are robust to the noise in the volatility proxy. We consider the *MSE* and *QLIKE* ratios, defined respectively as

$$rMSE = \frac{MSE_i}{MSE_{HAR}} \quad rQLIKE = \frac{QLIKE_i}{QLIKE_{HAR}}, \quad (12)$$

⁵The *QLIKE* index is computed as average of a simple modification of the familiar Gaussian log-likelihood loss function, which belongs to the family of robust and homogeneous loss functions defined by Patton (2011b), with parameter $b = -2$. The modification is such that the index amounts to zero when $\widehat{RV}_t = RV_t$, that is, the daily observed *RV* is forecast without error (Patton and Sheppard, 2009, Patton, 2011a). It gives asymmetric weights to the forecast errors, so that underestimating the *RV* is more important than overestimating.

where MSE_i ($QLIKE_i$) is defined as the forecast MSE ($QLIKE$) over the out-of-sample period of any of our competing models, and MSE_{HAR} ($QLIKE_{HAR}$) is the respective value of the HAR benchmark model. The values less than 1 are associated with the superior forecast ability of the proposed model, and vice versa.

In order to examine the advantages of the individual HAR models and the HAR models with forecast reconciliation methods over the HAR benchmark model, we then employ the Diebold and Mariano (1995) test (DM test) to investigate the null hypothesis of equal predict accuracy (EPA) where the HAR model is used as a benchmark.

Finally, we utilize the Model Confidence Set (MCS) approach developed by Hansen et al. (2011) to compare the point forecast accuracy between the direct daily forecasts and the reconciliation-based forecasts using intraday decompositions of RV . Given a set of candidate forecast models, \mathcal{M}_0 , the goal of the MCS procedure is to identify the MCS $\hat{\mathcal{M}}_{1-\alpha}^* \subset \mathcal{M}_0$, which is the set of the models that contains the “best” forecast model given a level of confidence α . The MCS procedures start with the full set of models $\mathcal{M} = \mathcal{M}_0 = \{1, \dots, m_0\}$ and repeatedly test the null hypothesis of EPA:

$$H_{0,\mathcal{M}} : E(d_{ij,t}) = 0, \quad \forall i, j \in \mathcal{M} \quad (13)$$

where $d_{ij,t} = \mathcal{L}_{i,t} - \mathcal{L}_{j,t}$ is the loss differential between models i and j in the set⁶. The MCS procedure sequentially eliminates the worst performance model from \mathcal{M} , as long as the null is rejected at the significance level of α . This trimming of models is repeated until the null is not rejected any longer, and the surviving set of models form the MCS, $\hat{\mathcal{M}}_{1-\alpha}^*$. If a fixed significance level of α is used at each step, $\hat{\mathcal{M}}_{1-\alpha}^*$ contains the best model from $\hat{\mathcal{M}}$ with $(1 - \alpha)$ confidence.

Hansen et al. (2011) present three different types of statistics for testing the EPA hy-

⁶The loss function \mathcal{L} is either MSE or $QLIKE$.

pothesis. We employ the MCS procedure based on the t -statistics

$$t_{ij} = \frac{\bar{d}_{ij}}{\sqrt{\widehat{var}(\bar{d}_{ij})}} \quad \text{for } i, j \in \mathcal{M}, \quad (14)$$

where $\bar{d}_{ij} = \frac{1}{T_h} \sum_{t=N}^{T-h} d_{ij,t}$. The quantity t_{ij} , provides scaled information on the average difference in the point forecast quality of models i and j . $\widehat{var}(\bar{d}_{ij})$ is an estimate of $var(\bar{d}_{ij})$, obtained by using the stationary block bootstrap of Politis and Romano (1994) following Hansen et al. (2011). The range statistics T_R is given by

$$T_R = \max_{i,j \in \mathcal{M}} |t_{ij}| = \max_{i,j \in \mathcal{M}} \frac{|\bar{d}_{ij}|}{\sqrt{\widehat{var}(\bar{d}_{ij})}}. \quad (15)$$

The MCS procedure assigns p -values to each model in the initial set. For a given model $i \in \mathcal{M}$, the MCS p -value, \hat{p}_i , is the threshold confidence level that determines whether the model belongs to the MCS. It holds that $\widehat{\mathcal{M}}_{1-\alpha}^*$ if and only if $\hat{p}_i \geq \alpha$.

5 Does forecast reconciliation help in RV forecasting?

Our final purpose is to answer the following question: when ‘volatility-based’ decompositions of the daily realized volatility are available, does considering forecast reconciliation significantly improve the forecast accuracy of daily RV compared to the benchmark HAR -type models by Corsi (2009), Patton and Sheppard (2015) and Bollerslev et al. (2022)?

We start by evaluating the direct forecasts accuracy for the DJIA using the MSE and $QLIKE$ ratios (Table 4, Panel A). First of all, it appears that the benchmark HAR model is almost always outperformed by both SV and $PV(3)$ in terms of $QLIKE$, the only exception being for $h = 1$. On the contrary, $h = 1$ and $PV(3)$ model is the only combination forecast horizon/model at which the HAR model is outperformed in terms of MSE . Second, the $QLIKE$ indices of the forecast reconciliation-based approaches, either indirect (bu) or regression-based (shr), improve on both the HAR benchmark model (apart SV_{bu} at $h = 1$)

	MSE			QLIKE		
	$h = 1$	$h = 5$	$h = 22$	$h = 1$	$h = 5$	$h = 22$
<i>Panel A: DJIA index</i>						
SV	1.028	1.017	1.003	0.973	0.997	0.928
SV_{bu}	0.960	0.972	1.005	1.010	0.237	0.748
SV_{shr}	0.976	0.991	1.002	0.983	0.233	0.728
$PV(3)$	0.816	1.077	1.025	2.272	0.977	0.962
$PV(3)_{bu}$	0.924	0.957	1.009	1.001	0.235	0.596
$PV(3)_{shr}$	0.833	1.015	1.015	0.945	0.225	0.596
<i>Panel B: Individual stocks</i>						
SV	1.016	1.008	1.001	1.092	0.998	0.993
SV_{bu}	0.964	0.992	0.998	0.921	0.977	0.971
SV_{shr}	0.980	0.996	0.998	0.899	0.947	0.960
$PV(3)$	0.899	0.976	1.010	1.364	1.025	1.055
$PV(3)_{bu}$	0.943	0.982	0.995	0.900	0.895	0.945
$PV(3)_{shr}$	0.896	0.964	0.994	0.833	0.824	0.916

Table 4: Forecast accuracy at forecast horizons $h = 1, 5, 22$. *MSE* and *QLIKE* ratios over the benchmark *HAR* model for the DJIA index (panel A), and geometric means of the *MSE* and *QLIKE* ratios for individual stocks (panel B). Values larger than one are highlighted in red. The best index value in each column is highlighted in bold.

and their direct counterparts. Again, this picture is not confirmed by the *MSE* indices, because of the different view at the forecasting accuracy offered by these two indices.

The individual stocks' forecast performance analysis (Table 4, Panel B) provides more compelling findings. We note that considering very simple intraday decompositions of RV_t in a forecast-reconciliation framework, either indirect (i.e., SV_{bu} and $PV(3)_{bu}$), or regression-based (i.e., SV_{shr} and $PV(3)_{shr}$), always improves on the forecasting accuracy of the *HAR* benchmark model: both *MSE* and *QLIKE* are less than one at any forecast horizon. In addition, SV_{shr} and $PV(3)_{shr}$ always improve on their direct forecasting approaches counterparts, at any forecast horizon and in terms of both *MSE* and *QLIKE* indices, with the most notable results being offered by $PV(3)_{shr}$, which stably gives the best accuracy indices (highlighted in bold in Table 4, Panel B).

Following Hansen et al. (2011), we implement the MCS procedure using the block bootstrap of Politis and Romano (1994) (see Hansen, 2005), in which blocks have length of 22 days, and results are based on 10,000 resamples. We choose both the *MSE* and the *QLIKE* loss functions, and use the test statistic T_{max} to test the null hypothesis of no difference be-

tween the forecast accuracy of the considered model. The results for the forecast horizons $h = 1, 5, 22$ are shown in Tables 5, 6 and 7, respectively.

For the DJIA index, results sensibly differ between *MSE* and *QLIKE*, coherently with Table 4: while for *MSE* the MCS includes all models (apart SV_{bu} for $h = 5$), in the case of *QLIKE*, $PV(3)_{shr}$ is the best model at $h = 1$ and $h = 5$ (for $h = 22$ even under *QLIKE* most models are equivalent). For the Diebold-Mariano test, under *MSE* only few cases lead to a rejection of the null hypothesis, while with *QLIKE* for $h = 5$ and $h = 22$ the models with forecast reconciliation improves over the benchmark models in a statistically significant way in most cases. Moving to the individual stocks, we stress that Tables 5, 6 and 7 report aggregated results, thus providing an overall evaluation in the cross-section of the 26 stocks. We highlight that even in this case performances differ between *MSE* and *QLIKE*: for the former, improvements are limited and only in few cases we do have rejections of the null for the Diebold-Mariano test, or models excluded from the confidence set; for the latter, the use of forecast reconciliation leads to a clear improvement, with $PV(3)_{shr}$ providing, overall, better performances.

These evidences are confirmed and enriched by Figure 4, which shows the results of the Multiple Comparison with the Best (MCB) Nemenyi test, a non-parametric multiple comparison procedure frequently adopted in the forecasting literature (see Koning et al., 2005, Kourentzes and Athanasopoulos, 2019, and Makridakis et al., 2022, among others). In particular, the single model $PV(3)$ does not significantly improve on the benchmark *HAR* (the corresponding lines in the ‘Multiple Comparison with the Best’ graphs for both *MSE* and *QLIKE* are overlapping). Further, the forecasts produced by the $PV(3)_{shr}$ approach are significantly better than the benchmarks *HAR* and *SV*, both in terms of *MSE* and *QLIKE*, while direct $PV(3)$ forecasts appear significantly worse if the *QLIKE* loss function is used to evaluate the forecast accuracy. Finally, overall $PV(3)_{shr}$ shows the best forecast accuracy: it is not significantly worse than $PV(3)_{bu}$, the most performing approach in terms of *MSE*, and ranks first in terms of *QLIKE*, while SV_{shr} is the only approach with a statistically

	RV	SV	$PV(3)$	SV_{bu}	$PV(3)_{bu}$	SV_{shr}	$PV(3)_{shr}$
<i>Panel A: DJIA index</i>							
MSE	6.352	6.527	5.184	6.099	5.867	6.202	5.293
p -value dm_{RV}	—	0.785	0.168	0.142	0.075	0.119	0.066
p -value dm_{SV}	—	—	0.131	0.148	0.079	0.115	0.044
p -value dm_{PV}	—	—	—	0.800	0.759	0.821	0.579
p -value MCS	0.264	0.224	1.000	0.358	0.431	0.292	0.713
$QLIKE$	0.216	0.210	0.491	0.218	0.217	0.212	0.204
p -value dm_{RV}	—	0.004	0.908	0.692	0.528	0.176	0.008
p -value dm_{SV}	—	—	0.911	0.988	0.956	0.796	0.031
p -value dm_{PV}	—	—	—	0.098	0.097	0.093	0.087
p -value MCS	0.155	0.122	0.192	0.030	0.162	0.028	1.000
<i>Panel B: Individual stocks</i>							
MSE	39.595	40.993	36.374	37.805	36.947	38.970	35.553
p -value dm_{RV}	—	0	0	1	2	1	2
p -value dm_{SV}	—	—	0	0	1	5	2
p -value dm_{PV}	—	—	—	1	1	2	1
p -value MCS	23	19	26	20	25	22	26
$QLIKE$	0.185	0.214	0.269	0.170	0.165	0.165	0.151
p -value dm_{RV}	—	2	1	2	4	7	19
p -value dm_{SV}	—	—	1	6	7	10	20
p -value dm_{PV}	—	—	—	7	8	8	10
p -value MCS	10	8	19	6	4	6	26

Table 5: *One-day-ahead forecasting performance: 2007-2022 (3,880 days)*

Note: The table reports the **1-step ahead** forecasting performance of the different models. The top panel shows the results for the DJIA index, while the bottom panel refers to individual stocks. MSE and $QLIKE$ refer to the loss function value for a given model (top panel) or average loss function across individual stocks (bottom panel). The one-sided tests between each forecasting model against HAR , SV , and $PV(3)$ are denoted by dm_{HAR} , dm_{SV} , and $dm_{PV(3)}$, respectively. The top panel includes p-values while the bottom panel reports 5% rejection frequencies. MCS denotes the p -value of that model being in the Model Confidence Set (top panel), or the number of times that model is in the 80% Model Confidence Set (lower panel). $PV(3)$ uses three intraday decompositions defined by two thresholds at 10% and 75%. In the upper panel we highlight in bold p -values < 0.05 for Diebold-Mariano and p -values > 0.2 for MCS. In the both panel we highlight in bold the minimum (average) loss function.

	RV	SV	$PV(3)$	SV_{bu}	$PV(3)_{bu}$	SV_{shr}	$PV(3)_{shr}$
<i>Panel A: DJIA index</i>							
MSE	5.109	5.195	5.503	4.966	4.888	5.064	5.185
p -value dm_{RV}	—	0.774	0.833	0.021	0.007	0.235	0.613
p -value dm_{SV}	—	—	0.783	0.054	0.023	0.049	0.485
p -value dm_{PV}	—	—	—	0.105	0.077	0.139	0.027
p -value MCS	0.408	0.369	0.369	0.090	1.000	0.288	0.443
$QLIKE$	0.930	0.927	0.908	0.220	0.219	0.217	0.209
p -value dm_{RV}	—	0.000	0.441	0.008	0.008	0.008	0.007
p -value dm_{SV}	—	—	0.449	0.008	0.008	0.008	0.007
p -value dm_{PV}	—	—	—	0.007	0.007	0.007	0.006
p -value MCS	0.462	0.486	0.140	0.006	0.104	0.016	1.000
<i>Panel B: Individual stocks</i>							
MSE	25.109	25.371	22.936	24.804	24.433	24.923	22.753
p -value dm_{RV}	—	0	1	2	9	4	2
p -value dm_{SV}	—	—	1	2	4	4	3
p -value dm_{PV}	—	—	—	0	0	0	0
p -value MCS	26	22	26	25	26	24	26
$QLIKE$	0.186	0.187	0.201	0.181	0.161	0.174	0.147
p -value dm_{RV}	—	6	7	4	8	9	24
p -value dm_{SV}	—	—	7	2	4	3	21
p -value dm_{PV}	—	—	—	2	4	2	8
p -value MCS	11	13	22	9	6	9	24

Table 6: Five-day-ahead forecasting performance: 2007-2022 (3,880 days)

Note: The table reports the **1-step ahead** forecasting performance of the different models. The top panel shows the results for the DJIA index, while the bottom panel refers to individual stocks. MSE and $QLIKE$ refer to the loss function value for a given model (top panel) or average loss function across individual stocks (bottom panel). The one-sided tests between each forecasting model against HAR , SV , and $PV(3)$ are denoted by dm_{HAR} , dm_{SV} , and $dm_{PV(3)}$, respectively. The top panel includes p-values while the bottom panel reports 5% rejection frequencies. MCS denotes the p -value of that model being in the Model Confidence Set (top panel), or the number of times that model is in the 80% Model Confidence Set (lower panel). $PV(3)$ uses three intraday decompositions defined by two thresholds at 10% and 75%. In the upper panel we highlight in bold p -values < 0.05 for Diebold-Mariano and p -values > 0.2 for MCS. In the lower panel we highlight in bold the minimum (average) loss function.

	RV	SV	$PV(3)$	SV_{bu}	$PV(3)_{bu}$	SV_{shr}	$PV(3)_{shr}$
<i>Panel A: DJIA index</i>							
MSE	4.424	4.436	4.533	4.448	4.463	4.434	4.488
p -value dm_{RV}	—	0.613	0.851	0.631	0.683	0.569	0.780
p -value dm_{SV}	—	—	0.843	0.575	0.646	0.478	0.765
p -value dm_{PV}	—	—	—	0.209	0.257	0.158	0.225
p -value MCS	1.000	0.869	0.727	0.841	0.841	0.761	0.811
$QLIKE$	0.973	0.902	0.936	0.727	0.580	0.708	0.580
p -value dm_{RV}	—	0.160	0.150	0.027	0.002	0.016	0.002
p -value dm_{SV}	—	—	0.830	0.049	0.004	0.028	0.003
p -value dm_{PV}	—	—	—	0.031	0.002	0.017	0.002
p -value MCS	0.314	0.437	0.453	0.135	1.000	0.323	0.951
<i>Panel B: Individual stocks</i>							
MSE	14.243	14.277	14.316	14.205	14.231	14.207	14.122
p -value dm_{RV}	—	1	2	2	4	3	3
p -value dm_{SV}	—	—	2	1	2	2	2
p -value dm_{PV}	—	—	—	3	2	3	6
p -value MCS	24	24	24	24	25	23	24
$QLIKE$	0.269	0.268	0.292	0.262	0.255	0.259	0.247
p -value dm_{RV}	—	5	6	4	10	6	22
p -value dm_{SV}	—	—	5	3	6	4	17
p -value dm_{PV}	—	—	—	8	10	9	14
p -value MCS	18	19	24	13	15	13	24

Table 7: *Twenty-two-day-ahead forecasting performance: 2007-2022 (3,880 days)*

Note: The table reports the **1-step ahead** forecasting performance of the different models. The top panel shows the results for the DJIA index, while the bottom panel refers to individual stocks. MSE and $QLIKE$ refer to the loss function value for a given model (top panel) or average loss function across individual stocks (bottom panel). The one-sided tests between each forecasting model against HAR , SV , and $PV(3)$ are denoted by dm_{HAR} , dm_{SV} , and $dm_{PV(3)}$, respectively. The top panel includes p-values while the bottom panel reports 5% rejection frequencies. MCS denotes the p -value of that model being in the Model Confidence Set (top panel), or the number of times that model is in the 80% Model Confidence Set (lower panel). $PV(3)$ uses three intraday decompositions defined by two thresholds at 10% and 75%. In the upper panel we highlight in bold p -values < 0.05 for Diebold-Mariano and p -values > 0.2 for MCS. In the lower panel we highlight in bold the minimum (average) loss function.

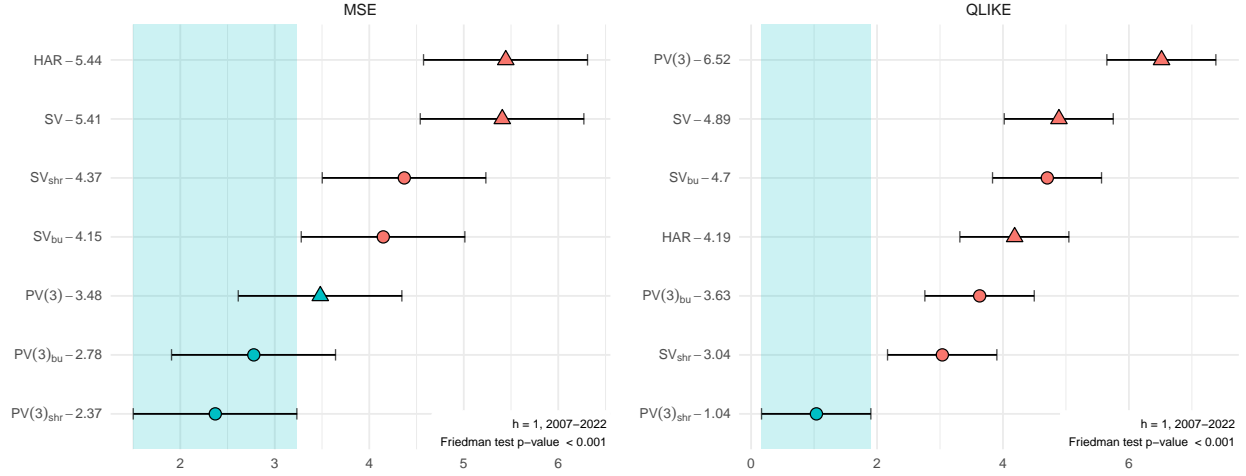


Figure 4: MCB Nemenyi test results: average ranks and 95% confidence intervals for the **one-step ahead** RV forecasts of the DJIA index and 26 individual stocks. Direct daily RV forecasts from HAR, SV and PV(3) models, and from their extensions with the bottom-up (bu) and the MinT-shr (shr) forecast reconciliation-based approaches according to the corresponding intraday RV decomposition. The forecasting approaches are sorted vertically according to the MSE mean rank (left panel) and the QLIKE mean rank (right panel). The mean rank of each method is displayed to the right of their names. If the intervals of two forecasting models do not overlap, this indicates a statistically different performance. Thus, methods that do not overlap with the light blue interval are considered significantly worse than the best and vice-versa.

equivalent forecasting accuracy.

Further insights are offered in a simple, but effective descriptive view, by Figure 5, where the scatter plots of the 27 couples of, respectively, MSE and $QLIKE$ indices obtained using the benchmark HAR model and $PV(3)_{shr}$ are represented. It emerges that $PV(3)_{shr}$ outperforms the benchmark HAR in the majority of cases (23 out of 27) in terms of MSE , and always if $QLIKE$ is used to evaluate the forecasting accuracy. This consideration is somehow extended, and further supported, by the results shown in Figure 6, which contains a summary view of the number of times each forecasting approach provided better forecasting accuracy than the other procedures considered in the comparison. Summarizing, $PV(3)_{shr}$ registers a better prediction performance than all other approaches, with success rates in terms of $QLIKE$ ranging from 96.3% (26 of 27) to 100% (27 of 27), and from 55.6% (15 of 27) to 88.9% (24 of 27) if MSE is used.

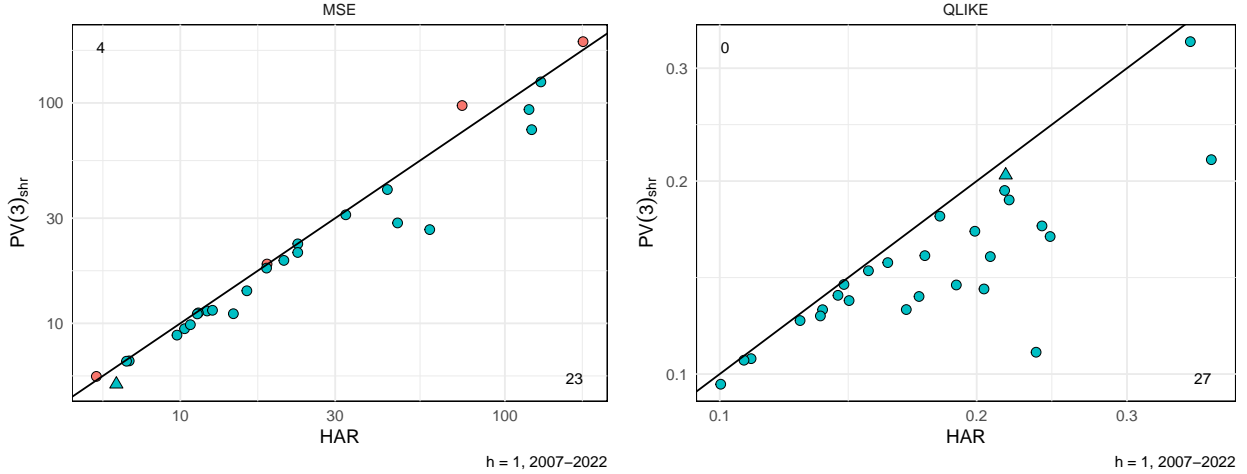


Figure 5: Accuracy of the *one-step ahead* daily RV forecasts for the DJIA index (triangle) and 26 individual stocks (circle) in terms of MSE (left panel) and QLIKE (right panel) indices. Comparison between HAR direct and $PV(3)_{shr}$ reconciliation-based forecasts. The black line represents the bisector, where either MSE's or QLIKE's for both approaches are equal. On the top-left (bottom-right) corner of each graph, the number of points above (below) the bisector is reported.

6 Robustness of the results

6.1 Sub-sample analysis

The interpretation of the results so far can be further detailed and specified by considering 4 different time windows of the complete 2007-2022 interval previously analysed, namely: 2006-2010, 2011-2014, 2015-2019, 2020-2022 (see Appendix 2). We observe that the predictive performance of models that make use of intraday decompositions in a reconciliation framework is constantly better in periods of high market volatility (2007-2010 and 2020-2022), while they do not worsen the predictive accuracy of the benchmark in the period 2015-2019, which is characterized by lower variances. The remaining period 2011-2014 offers different indications depending on whether one considers *QLIKE* or MSE. In the latter case, the $PV(3)$ model, both in the single version and in the version that makes use of forecast reconciliation, shows a better overall accuracy, although not significantly to the *HAR* benchmark.

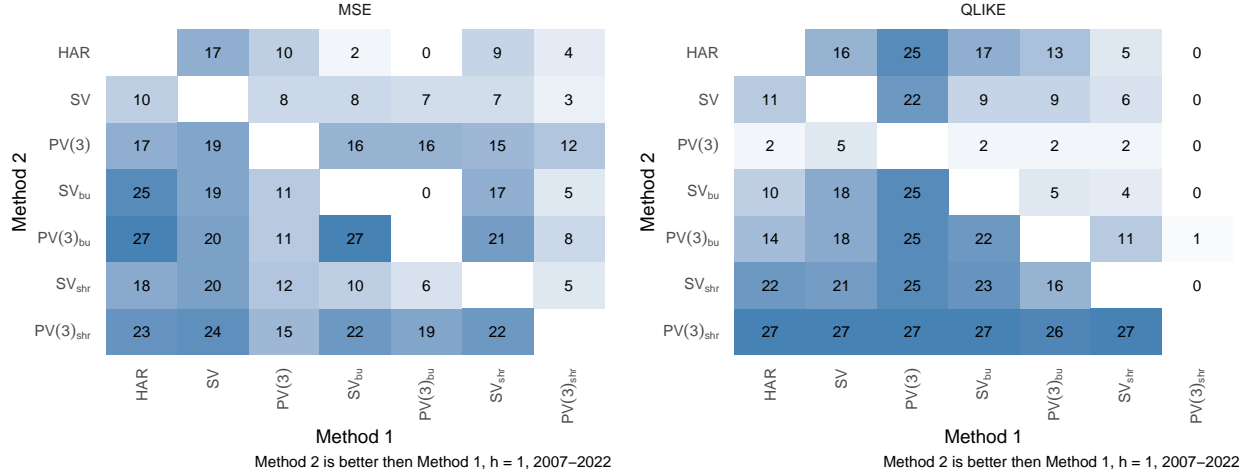


Figure 6: Qualitative evaluation of the *one-step ahead* forecasting accuracy. Each cell reports the number of times the forecasting model in the row outperforms the model in the column.

6.2 Grouped series

Here we consider the forecasting performance of reconciliation approaches applied to grouped time series defined by intraday RV decompositions based on time and returns' characteristics:

- TSV_{bu} : indirect (bottom-up) daily RV forecasts from ten bottom time series cross-classified by time interval and semi-variances;
- TSV_{shr} : two hierarchies sharing the ten bottom variables above, with eight upper variables;
- $TPV(3)_{bu}$: indirect (bottom-up) daily RV forecasts from fifteen bottom time series cross-classified by time interval and partial variances;
- TPV_{shr} : two hierarchies sharing the fifteen bottom variables above, with nine upper variables.

From Table 8 it appears that the regression-based reconciliation approach $TPV(3)_{shr}$ largely benefits from the adoption of a time decomposition (all indices are less than one). However, looking at Figure 7, $TPV(3)_{shr}$ gives results largely similar to those of the simpler $PV(3)_{shr}$ approach, that does not make use of any temporal decomposition.

	MSE			QLIKE		
	$h = 1$	$h = 5$	$h = 22$	$h = 1$	$h = 5$	$h = 22$
<i>Panel A: DJIA index</i>						
TSV_{bu}	0.824	0.801	1.099	1.085	0.249	0.385
TSV_{shr}	0.869	0.878	0.965	1.011	0.236	0.379
$TPV(3)_{bu}$	0.822	0.795	1.103	1.090	0.250	0.386
$TPV(3)_{shr}$	0.808	0.925	0.939	0.971	0.227	0.374
<i>Panel B: Individual stocks</i>						
TSV_{bu}	0.991	1.054	1.019	0.893	0.908	0.875
TSV_{shr}	0.987	1.007	0.984	0.850	0.861	0.853
$TPV(3)_{bu}$	0.982	1.039	1.012	0.894	0.902	0.868
$TPV(3)_{shr}$	0.924	0.967	0.965	0.805	0.793	0.824

Table 8: Forecast accuracy at forecast horizons $h = 1, 5, 22$. MSE and QLIKE ratios over the benchmark HAR model for the DJIA index (panel A), and geometric means of the MSE and QLIKE ratios for individual stocks (panel B). Values larger than one are highlighted in red. The best index value in each column is highlighted in bold.

6.3 An alternative PV decomposition

In the $PV(3)$ decomposition, the use of RV_t in the standardization of intraday returns exposes the estimators of standardized returns quantile to the influence of price jumps (i.e., extreme positive or negative returns) and of the intraday volatility pattern.

We consider here a slight modification in the construction of the decomposition by employing the contribution of Boudt et al. (2011) and exploiting a result of Andersen et al. (2007b). The former provide a methodology for estimating and filtering out the intraday variance pattern while the latter shows that, in large sample, the intraday returns standardized by the Bi-power variation follow an asymptotically normal distribution. We combine these two elements as follows. First, we compute returns filtered from the intraday volatility pattern by adopting the *WDS* approach of Boudt et al. (2011). The filtered returns are defined as $r_{i,t}^* = \frac{r_{i,t}}{\sigma_i}$ where σ_i is the intraday volatility at interval i , estimated with the *WDS* approach. Then, we evaluate the Bi-power variation, a jump-robust estimator of the integrated volatility, on the filtered returns: $\widetilde{BPV}_t = \frac{\pi}{2} \frac{N}{N-1} \sum_{i=2}^M |r_{i,t}^*| |r_{i,t}^*|$. Finally, we assume

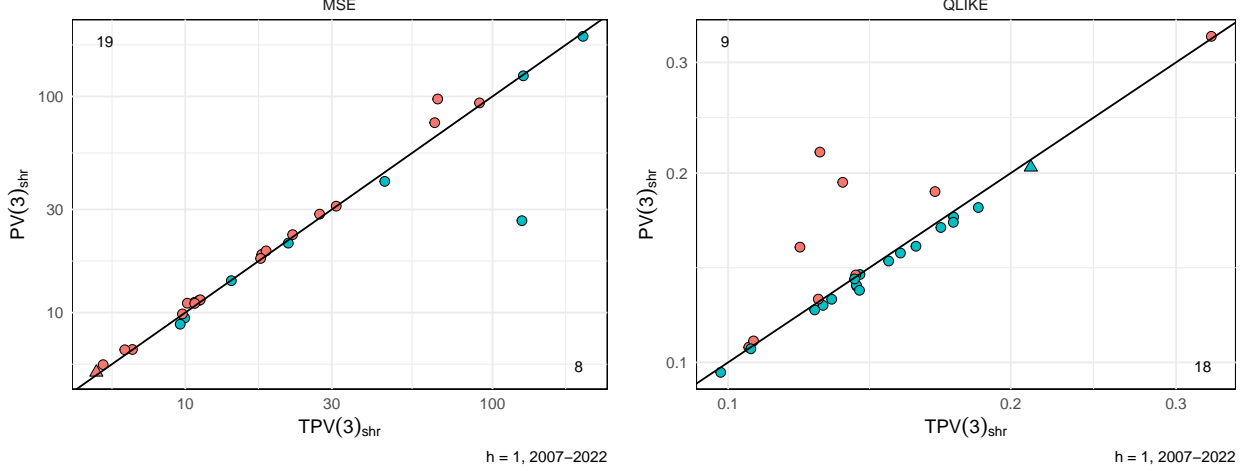


Figure 7: Accuracy of the *one-step ahead* daily RV forecasts for the DJIA index (triangle) and 26 individual stocks (circle) in terms of MSE (left panel) and QLIKE (right panel) indices. Comparison between HAR direct and $PV(3)_{shr}$ reconciliation-based forecasts. The black line represents the bisector, where either MSE's or QLIKE's for both approaches are equal. On the top-left (bottom-right) corner of each graph, the number of points above (below) the bisector is reported.

the following distribution for the filtered and standardized returns

$$\frac{r_{i,t}}{\sigma_i \sqrt{N^{-1} \widetilde{BPV}_t}} \sim \mathcal{N}(0, 1), \quad (16)$$

This quantity has already been used in Boudt et al. (2011) for jump detection. Going back to the PV framework, the empirical quantiles of standardized returns might be replaced by theoretical quantiles of the asymptotic distribution leading to

$$\tilde{c}_{i,t,j} = \sigma_i \sqrt{N^{-1} \widetilde{BPV}_t} \Phi^{-1}(\tau_j), \quad j = 1, 2, \dots, p-1. \quad (17)$$

Finally, we note that thresholds are both day-specific and intra-day-interval-specific. Similarly to the $PV(3)$, we now define a $PV(3)^*$ decomposition where we employ the previously defined quantiles with $\tau_1 = 0.1$ and $\tau_2 = 0.75$.

In Figure 8 the MSE and $QLIKE$ indices for the bottom-up reconciliations in the two cases are shown. It clearly appears that no meaningful accuracy improvement is obtained for the considered assets, and this turns out to be confirmed by Figure 9, where the regression-

based reconciliation approaches in the two cases are considered.

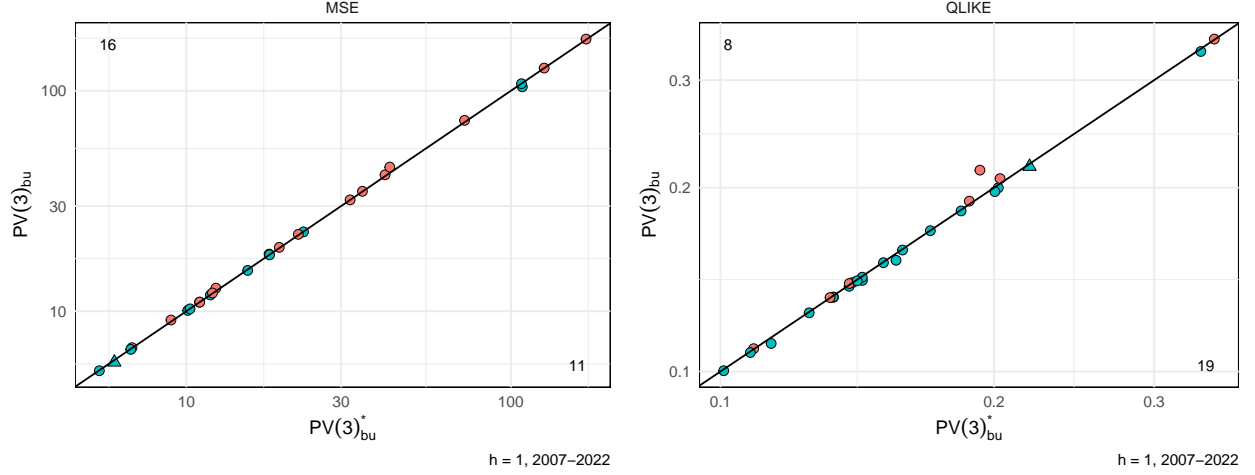


Figure 8: Accuracy of the *one-step ahead* daily RV forecasts for the DJIA index (triangle) and 26 individual stocks (circle) in terms of MSE (left panel) and QLIKE (right panel) indices. Comparison between HAR direct and $PV(3)_{shr}$ reconciliation-based forecasts. The black line represents the bisector, where either MSE's or QLIKE's for both approaches are equal. On the top-left (bottom-right) corner of each graph, the number of points above (below) the bisector is reported.

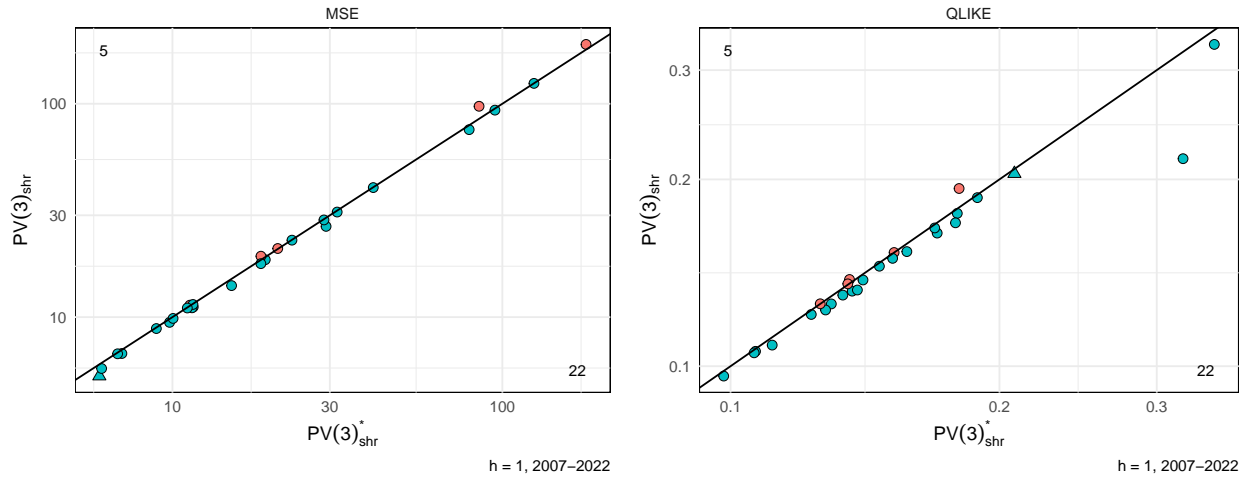


Figure 9: Accuracy of the *one-step ahead* daily RV forecasts for the DJIA index (triangle) and 26 individual stocks (circle) in terms of MSE (left panel) and QLIKE (right panel) indices. Comparison between HAR direct and $PV(3)_{shr}$ reconciliation-based forecasts. The black line represents the bisector, where either MSE's or QLIKE's for both approaches are equal. On the top-left (bottom-right) corner of each graph, the number of points above (below) the bisector is reported.

7 Concluding remarks

In this paper, we address whether using the disaggregate components of the daily realized volatility or combining them with the daily realized volatility forecasts improves the forecasting accuracy compared to using the daily realized volatility series alone. To this end, we investigate alternative ways of leveraging intraday RV decompositions in forecasting daily RV . The key question of this study is whether it is beneficial to model and forecast daily RV at the sub-component level, thus exploiting the informative content (from a forecasting point of view) of bottom time series, or whether a direct strategy should be preferred. The latter refers to the prediction of RV by directly modeling it, even when the explanatory variables include a decomposition of the RV itself. Differently, indirect (bottom-up) forecasting is based on the aggregation of models fit on the bottom series, whose forecasts are then aggregated to recover the prediction of the top series. Forecast reconciliation adds a further element, by restoring the aggregation constraints linking the bottom, possibly the intermediate, and the top-level time series. The idea is that an appropriate ‘imposition’ to the forecasts of the same constraints valid for the observed data should improve the overall forecasting accuracy. We obtain a forecast of different sub-components individually, and then combine them to estimate the forecast of the aggregated series in an indirect (bottom-up) and a reconciliation forecasting framework.

Our main results can be summarized as follows. Through a simple out-of-sample forecasting experiment, we show that both bottom-up and regression-based reconciliation procedures (Wickramasuriya et al., 2019) perform relatively well compared to the benchmark direct forecasting models by Corsi (2009), Patton and Sheppard (2015), and Bollerslev et al. (2022), mostly when the $PV(3)$ model by Bollerslev et al. (2022) is used to produce base forecasts of the daily RV top-level series. We find substantial and significant reductions in forecast errors when using the new proposed indirect/reconciliation approaches. The disaggregated procedures do quite well in forecasting RV , and the reconciliation approach is generally more promising. For the HAR model, the differences between the bottom-up and

the direct approach are clearly visible, and the regression-based reconciliation approach offers some additional improvements. This is somehow confirmed for both *SV* and *PV(3)* forecasts, where generally the combination scheme of single component models provides smaller forecast errors than both the indirect and direct forecasting approaches.

References

- Aït-Sahalia, Y., Cacho-Diaz, J., Laeven, R., 2015. Modeling financial contagion using mutually exciting jump processes. *Journal of Financial Economics* 117, 585–606. doi:10.1016/j.jfineco.2015.03.002.
- Aït-Sahalia, Y., Jacod, J., 2014. *High-Frequency Financial Econometrics*. Princeton: Princeton University Press.
- Andersen, T., Bollerslev, T., Diebold, F., 2007a. Roughing it up: Including jump components in the measurement, modeling, and forecasting of return volatility. *Review of Economics and Statistics* 89, 701–720. doi:10.1162/rest.89.4.701.
- Andersen, T., Bollerslev, T., Diebold, F., Ebens, H., 2001a. The distribution of realized stock return volatility. *Journal of Financial Economics* 61, 43–76. doi:10.1016/S0304-405X(01)00055-1.
- Andersen, T., Bollerslev, T., Diebold, F., Labys, P., 2001b. The distribution of realized exchange rate volatility. *Journal of the American Statistical Association* 96, 42–55. doi:10.1198/016214501750332965.
- Andersen, T., Bollerslev, T., Diebold, F., Labys, P., 2003. Modeling and forecasting realized volatility. *Econometrica* 71, 579–625. doi:10.1111/1468-0262.00418.
- Andersen, T., Bollerslev, T., Dobrev, D., 2007b. No-arbitrage semi-martingale restrictions for continuous-time volatility models subject to leverage effects, jumps and i.i.d. noise: Theory and testable distributional implications. *Journal of Econometrics* 138, 125–180. doi:10.1016/j.jeconom.2006.05.018.
- Andersen, T., Bollerslev, T., Huang, X., 2011. A reduced form framework for modeling volatility of speculative prices based on realized variation measures. *Journal of Econometrics* 160, 176–189. doi:10.1016/j.jeconom.2010.03.029.
- Barndorff-Nielsen, O., Kinnebrock, S., Shephard, N., 2010. Measuring downside risk: Realised semivariance. in: Bollerslev, T., Russel, J.R., Watson, M.W. (Eds.). *Volatility and Time Series Econometrics: Essays in Honor of Robert F. Engle*. Oxford: Oxford University Press, 117–136.
- Bollerslev, T., 2022. Realized semi(co)variation: Signs that all volatilities are not created equal. *Journal of Financial Econometrics* 20, 219–252. doi:10.1093/jfinec/nbab025.

- Bollerslev, T., Medeiros, M., Patton, A., Quaadvlieg, R., 2022. From zero to hero: Realized partial (co)variances. *Journal of Econometrics* 231, 348–360. doi:10.1016/j.jeconom.2021.04.013.
- Bollerslev, T., Patton, A., Quaadvlieg, R., 2016. Exploiting the errors: A simple approach for improved volatility forecasting. *Journal of Econometrics* 192, 1–18. doi:10.1016/j.jeconom.2015.10.007.
- Boudt, K., Croux, C., Laurent, S., 2011. Robust estimation of intraweek periodicity in volatility and jump detection. *Journal of Empirical Finance* 18, 353–367. doi:10.1016/j.jempfin.2010.11.005.
- Caporin, M., 2022. The role of jumps in realized volatility modeling and forecasting. *Journal of Financial Econometrics* nbab030. doi:<https://doi.org/10.1093/jjfinec/nbab030>.
- Corsi, F., 2009. A simple approximate long-memory model of realized volatility. *Journal of Financial Econometrics* 7, 174–196. doi:10.1093/jjfinec/nbp001.
- Corsi, F., Mitnik, S., Pigorsch, C., Pigorsch, U., 2008. The volatility of realized volatility. *Econometric Reviews* 27, 46–78. doi:10.1080/07474930701853616.
- Corsi, F., Renó, R., 2012. Discrete-time volatility forecasting with persistent leverage effect and the link with continuous-time volatility modeling. *Journal of Business and Economic Statistics* 30, 368–380. doi:10.1080/07350015.2012.663261.
- Di Fonzo, T., Girolimetto, D., 2023. Cross-temporal forecast reconciliation: Optimal combination method and heuristic alternatives. *International Journal of Forecasting* 39, 39–57. doi:10.1016/j.ijforecast.2021.08.004.
- Diebold, F., Mariano, R., 1995. Comparing predictive accuracy. *Journal of Business & Economic Statistics* 13, 253–63.
- Engle, R., 1982. Autoregressive conditional heteroskedasticity with estimates of the variance of united kingdom inflation. *Econometrica* 50, 987–1007. doi:10.2307/1912773.
- Frail, C., Marcellino, M., Mazzi, G.L., Proietti, T., 2011. Euromind: a monthly indicator of the euro area economic conditions. *Journal of the Royal Statistical Society. Series A* 174, 439–470. URL: 10.1111/j.1467-985X.2010.00675.x.
- Girolimetto, D., Di Fonzo, T., 2023a. Package FoReco: Point Forecast Reconciliation. Version 0.2.6. URL: <https://cran.r-project.org/package=FoReco>.
- Girolimetto, D., Di Fonzo, T., 2023b. Point and probabilistic forecast reconciliation for general linearly constrained multiple time series doi:10.48550/arXiv.2305.05330.
- Grassi, S., Proietti, T., Frail, C., Marcellino, M., Mazzi, G.L., 2015. Euromind-c: a disaggregate monthly indicator of economic activity for the euro area and member countries. *International Journal of Forecasting* 31, 712–738. doi:10.1016/j.ijforecast.2014.08.015.

- Hansen, P.R., 2005. A Test for Superior Predictive Ability. *Journal of Business and Economic Statistics* 23, 365–380. doi:10.1198/073500105000000063.
- Hansen, P.R., Lunde, A., Nason, J.M., 2011. The Model Confidence Set. *Econometrica* 79, 453–497. doi:10.3982/ECTA5771.
- Hyndman, R.J., Ahmed, R.A., Athanasopoulos, G., Shang, H.L., 2011. Optimal combination forecasts for hierarchical time series. *Computational Statistics and Data Analysis* 55, 2579–2589. doi:10.1016/j.csda.2011.03.006.
- Hyndman, R.J., Lee, A.J., Wang, E., 2016. Fast computation of reconciled forecasts for hierarchical and grouped time series. *Computational Statistics and Data Analysis* 97, 16–32. doi:10.1016/j.csda.2015.11.007.
- Koning, A.J., Franses, P.H., Hibon, M., Stekler, H., 2005. The M3 competition: Statistical tests of the results. *International Journal of Forecasting* 21, 397–409. doi:10.1016/j.ijforecast.2004.10.003.
- Kourentzes, N., Athanasopoulos, G., 2019. Cross-temporal coherent forecasts for Australian tourism. *Annals of Tourism Research* 75, 393–409. doi:10.1016/j.annals.2019.02.001.
- Makridakis, S., Spiliotis, E., Assimakopoulos, V., 2022. M5 accuracy competition: Results, findings, and conclusions. *International Journal of Forecasting* 38, 1346–1364. doi:10.1016/j.ijforecast.2021.11.013.
- Marcellino, M., Stock, J.H., Watson, M.W., 2003. Macroeconomic forecasting in the Euro area: country specific versus area-wide information. *European Economic Review* 47, 1–18. doi:10.1016/S0014-2921(02)00206-4.
- Mircetic, D., Rostami-Tabar, B., Nikolicic, S., Maslaric, M., 2022. Forecasting hierarchical time series in supply chains: an empirical investigation. *International Journal of Production Research* 60, 2514–2533. doi:10.1080/00207543.2021.1896817.
- Panagiotelis, A., Athanasopoulos, G., Gamakumara, P., Hyndman, R.J., 2021. Forecast reconciliation: A geometric view with new insights on bias correction. *International Journal of Forecasting* 37, 343–359. doi:10.1016/j.ijforecast.2020.06.004.
- Patton, A.J., 2011a. Data-based ranking of realised volatility estimators. *Journal of Econometrics* 161, 284–303. doi:10.1016/j.jeconom.2010.12.010.
- Patton, A.J., 2011b. Volatility forecast comparison using imperfect volatility proxies. *Journal of Econometrics* 160, 246–256. doi:10.1016/j.jeconom.2010.03.034.
- Patton, A.J., Sheppard, K., 2009. Optimal combination of realised volatility estimators. *International Journal of Forecasting* 25, 218–238. doi:10.1016/j.ijforecast.2009.01.011.
- Patton, A.J., Sheppard, K., 2015. Good volatility, bad volatility: Signed jumps and the persistence of volatility. *The Review of Economics and Statistics* 97, 683–697. doi:https://doi.org/10.1162/REST_a_00503.

- Petropoulos, F., Makridakis, S., Assimakopoulos, V., Nikolopoulos, K., 2014. ‘Horses for Courses’ in demand forecasting. *European Journal of Operational Research* 237, 152–163. doi:10.1016/j.ejor.2014.02.036.
- Politis, D., Romano, J., 1994. The stationary bootstrap. *Journal of the American Statistical Association* 89, 1303–1313. doi:10.2307/2290993.
- Poncela, P., García-Ferrer, A., 2014. The effects of disaggregation on forecasting nonstationary time series. *Journal of Forecasting* 33, 300–314. doi:10.1002/for.2291.
- Sévy, B., 2014. Forecasting the volatility of crude oil futures using intraday data. *European Journal of Operational Research* 235, 643–659. doi:10.1016/j.ejor.2014.01.019.
- Silva, F.L., Souza, R.C., Oliveira, F.L.C., Lourenco, P.M., Calili, R.F., 2018. A bottom-up methodology for long term electricity consumption forecasting of an industrial sector - Application to pulp and paper sector in Brazil. *Energy* 144, 1107–1118. doi:10.1016/j.energy.2017.12.078.
- Sohn, S.Y., Lim, M., 2007. Hierarchical forecasting based on AR-GARCH model in a coherent structure. *European Journal of Operational Research* 176, 1033–1040. doi:10.1016/j.ejor.2005.08.019.
- van Erven, T., Cugliari, J., 2015. Game-Theoretically Optimal Reconciliation of Contemporaneous Hierarchical Time Series Forecasts, in: Antoniadis, A., Poggi, J.M., Brossat, X. (Eds.), *Modeling and Stochastic Learning for Forecasting in High Dimensions*. Springer International Publishing, Cham. volume 217, pp. 297–317. doi:10.1007/978-3-319-18732-7_15.
- Wang, S., Deng, X., Chen, H., Shin, Q., Xu, D., 2021. A bottom-up short-term residential load forecasting approach based on appliance characteristic analysis and multi-task learning. *Electric Power Systems Research* 196, 107233. doi:10.1016/j.epsr.2021.107233.
- Wickramasuriya, S.L., Athanasopoulos, G., Hyndman, R.J., 2019. Optimal Forecast Reconciliation for Hierarchical and Grouped Time Series Through Trace Minimization. *Journal of the American Statistical Association* 114, 804–819. doi:10.1080/01621459.2018.1448825.

Exploiting Intraday Decompositions in Realized Volatility Forecasting: A Forecast Reconciliation Approach

APPENDIX

Massimiliano Caporin, Tommaso Di Fonzo, and Daniele Girolimetto
Department of Statistical Sciences, University of Padova

June 6, 2023

A1: Data description

A summary description of the daily RV s for the DJIA index and 26 individual stocks is in Table 1. Figures 1, 2, 3 show the time series of RV and its SV and $PV(3)$ components for the DJIA index, while the RV of the DJIA index for the 5 time intervals of the day are shown in Figure 4. The RV graphs for the individual stocks are shown in Figures 5, 6, 7.

Email: massimiliano.caporin@unipd.it (M.C.), tommaso.difonzo@unipd.it (T.D.F.),
daniele.girolimetto@phd.unipd.it (D.G.)

Ticker	Company	GICS* Sector	Min	Mean	Median	Max	St.dv.	Skew.	Kurt.
DJIA	<i>Dow Jones Industrial Average index</i>		0.020	0.937	0.382	105.107	2.655	17.016	525.675
AAPL	Apple Inc.	Information technology	0.122	3.231	1.899	167.230	5.729	12.440	256.828
AMGN	Amgen	Health Care	0.311	2.408	1.673	104.363	3.708	12.014	222.839
AXP	American Express	Financials	0.131	3.450	1.210	275.174	8.992	10.565	212.313
BA	Boeing	Industrials	0.187	3.147	1.566	336.957	8.591	20.090	598.972
CAT	Caterpillar Inc.	Industrials	0.217	3.017	1.704	167.521	5.463	10.647	212.560
CSCO	Cisco	Information technology	0.237	2.575	1.681	128.759	4.264	11.737	230.317
CVX	Chevron Corporation	Energy	0.219	2.316	1.264	212.251	5.488	16.986	498.805
DIS	Disney	Communication Services	0.168	2.399	1.349	163.579	4.587	13.627	355.131
GS	Goldman Sachs	Financials	0.204	3.622	1.614	468.029	12.412	22.562	709.009
HD	Home Depot (The)	Consumer Discretionary	0.163	2.581	1.344	364.037	7.350	29.328	1287.173
HON	Honeywell	Industrials	0.146	2.365	1.349	166.977	4.922	13.936	334.939
IBM	IBM	Information technology	0.140	1.604	0.916	103.611	3.403	12.103	236.646
INTC	Intel	Information technology	0.337	2.851	1.904	111.192	4.407	11.059	192.990
JNJ	Johnson & Johnson	Health Care	0.118	1.219	0.700	115.272	3.132	19.937	578.804
JPM	JPMorgan Chase	Financials	0.186	3.738	1.410	362.245	11.103	14.267	331.107
KO	The Coca-Cola Company	Consumer Staples	0.188	1.311	0.796	87.093	2.786	14.112	298.911
MCD	McDonald's	Consumer Discretionary	0.125	1.638	0.918	141.630	3.742	17.477	495.913
MMM	3M	Industrials	0.135	1.680	0.979	141.197	3.784	18.862	565.079
MRK	Merck	Health Care	0.242	2.154	1.215	171.104	4.636	16.048	440.157
MSFT	Microsoft	Information technology	0.089	2.162	1.353	80.692	3.495	9.640	143.703
NKE	Nike Inc.	Consumer Discretionary	0.208	2.321	1.249	189.811	4.891	16.803	500.581
PG	Procter & Gamble	Consumer Staples	0.152	1.404	0.733	658.769	10.002	58.625	3811.064
UNH	UnitedHealth Group	Health Care	0.227	3.115	1.592	198.469	6.953	12.739	271.191
VZ	Verizon	Communication Services	0.156	1.864	1.034	232.582	4.999	26.244	1046.776
WBA	Walgreens Boots Alliance	Consumer Staples	0.215	2.581	1.666	119.073	3.959	11.147	219.696
WMT	Walmart	Consumer Staples	0.127	1.464	0.890	122.954	2.974	19.248	635.463

* Global Index Classification Standard.

Table 1: Descriptive statistics of the (open-to-close) daily Realized Variances of the DJIA index and 26 individual stocks for the period January 2, 2003 - June 30, 2022 (4,908 daily observations).

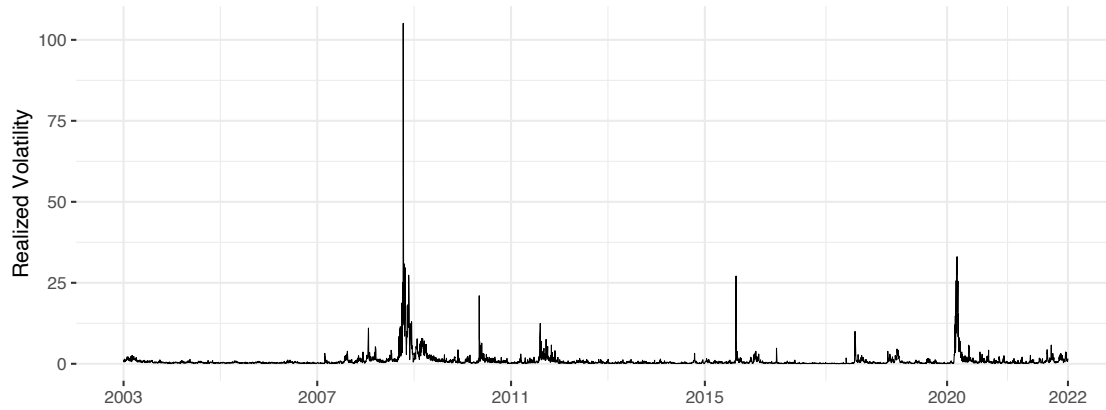


Figure 1: *DJIA index: daily Realized Variance, January 2, 2003 - June 30, 2022 (4,908 days).*

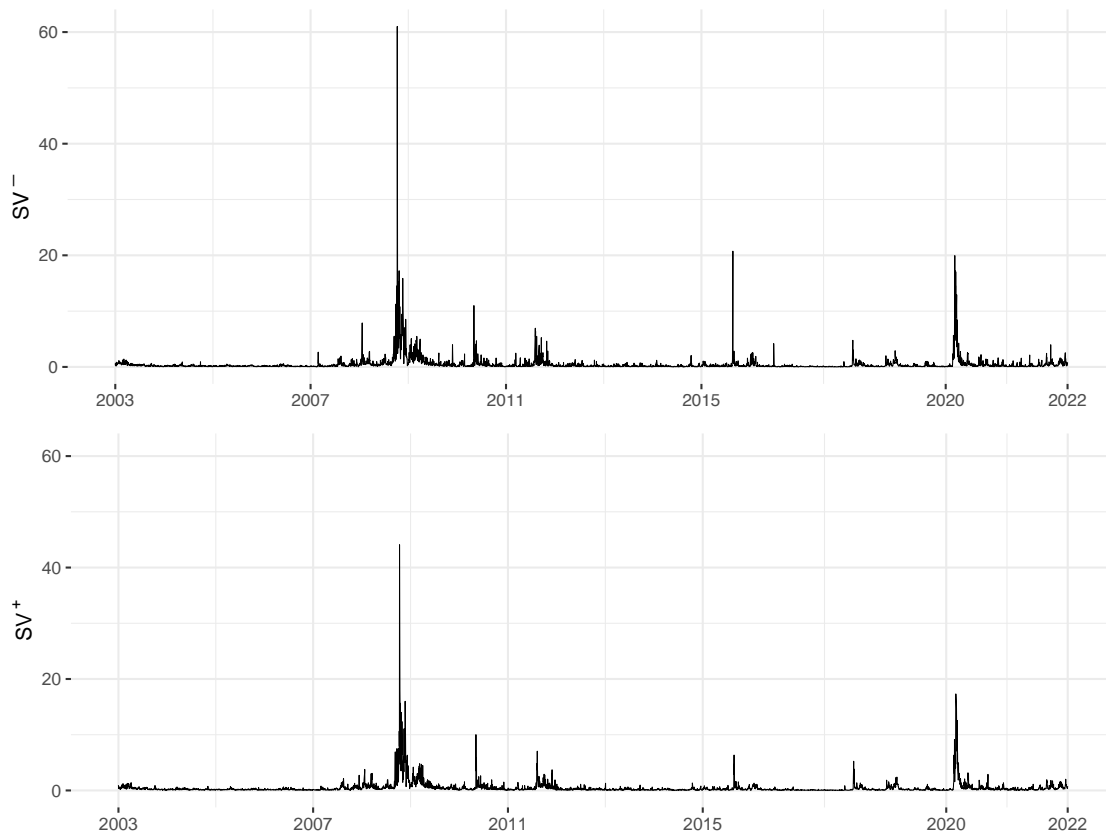


Figure 2: *DJIA index: daily Realized Semi-Variations, January 2, 2003 - June 30, 2022 (4,908 days).*

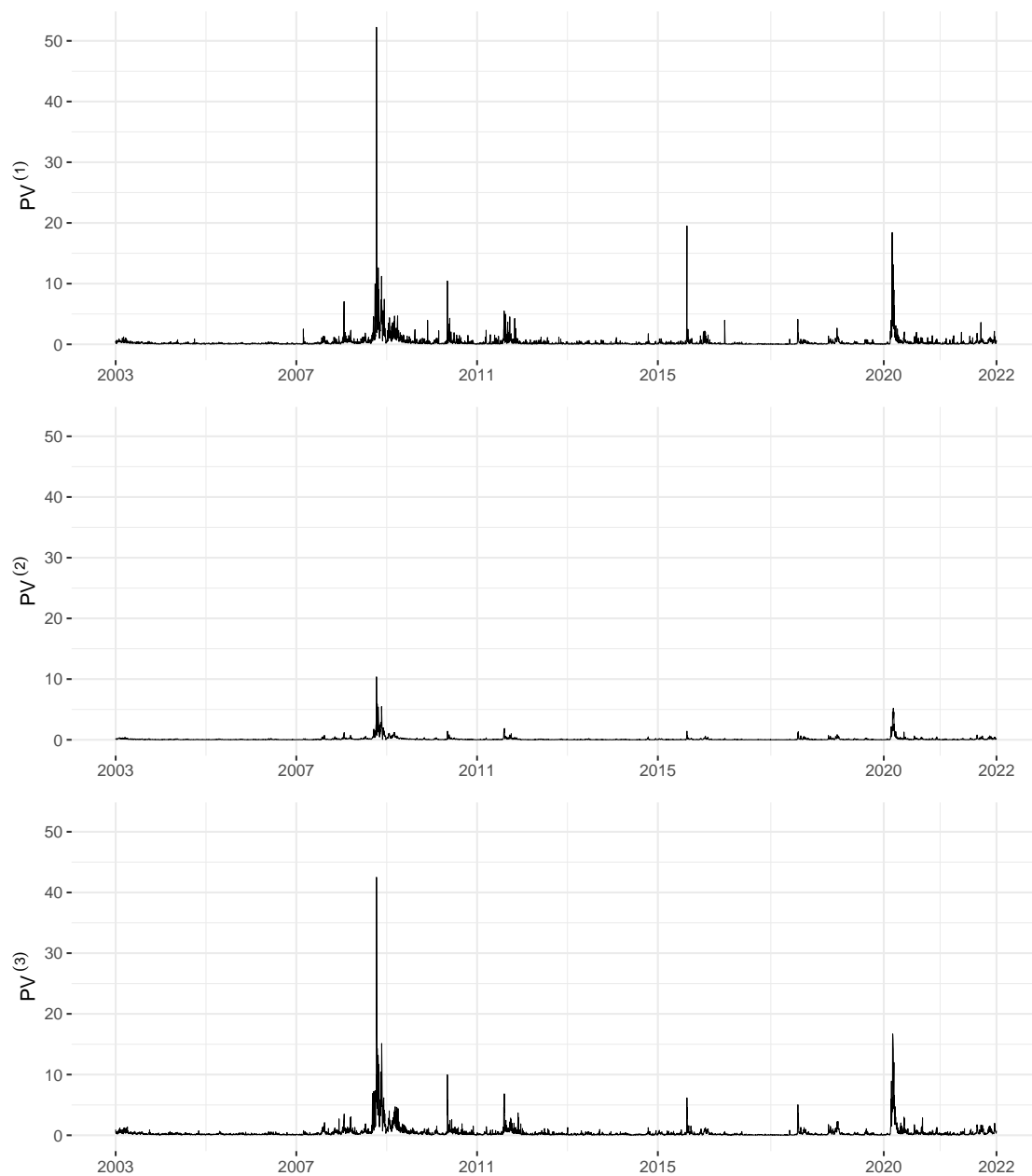


Figure 3: *DJIA index: daily Realized Power-Variances, January 2, 2003 - June 30, 2022 (4,908 days).*

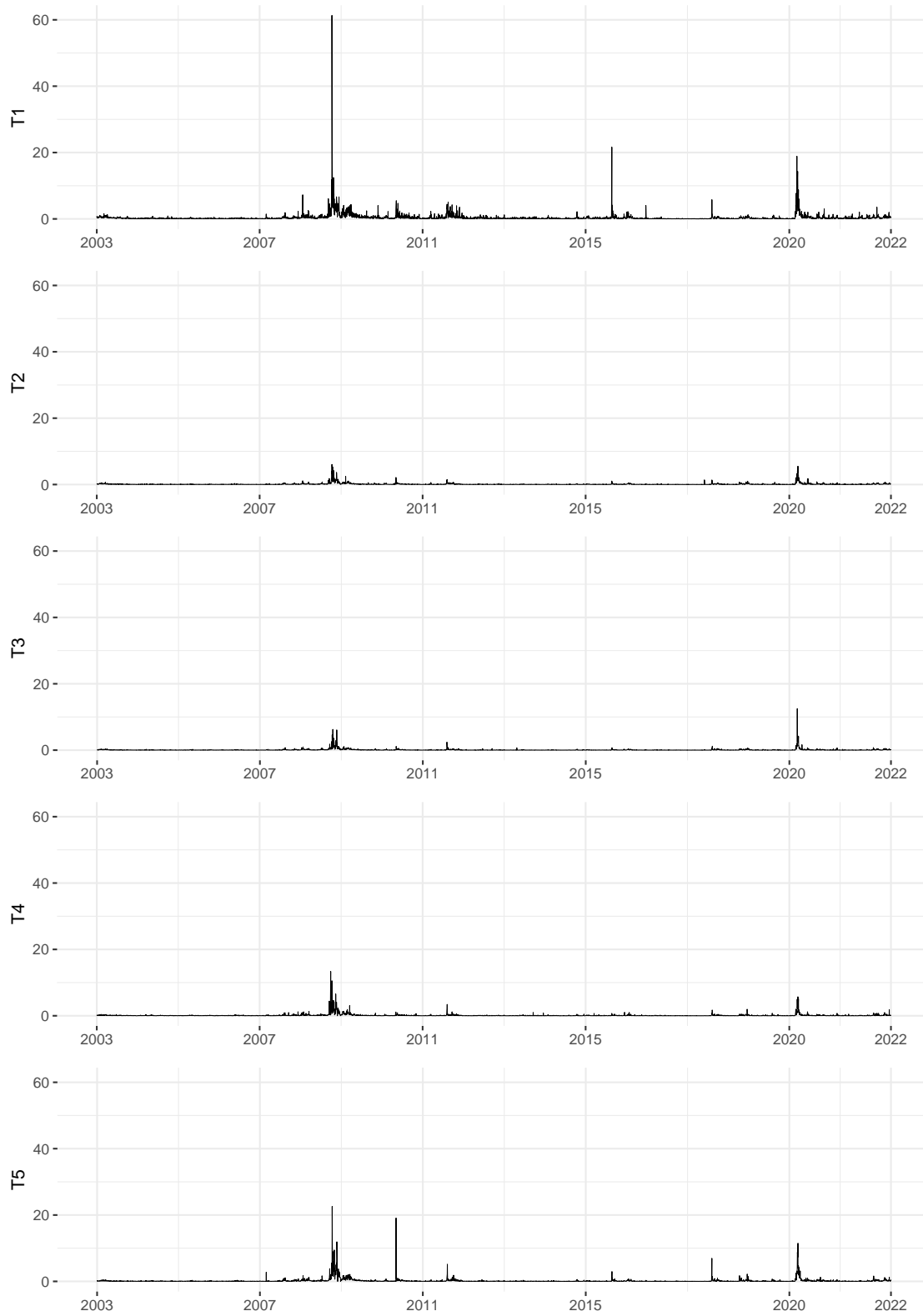


Figure 4: *DJIA index: Realized Variances in non-overlapping 78-minutes segments of the day, January 2, 2003 - June 30, 2022 (4,908 days).*

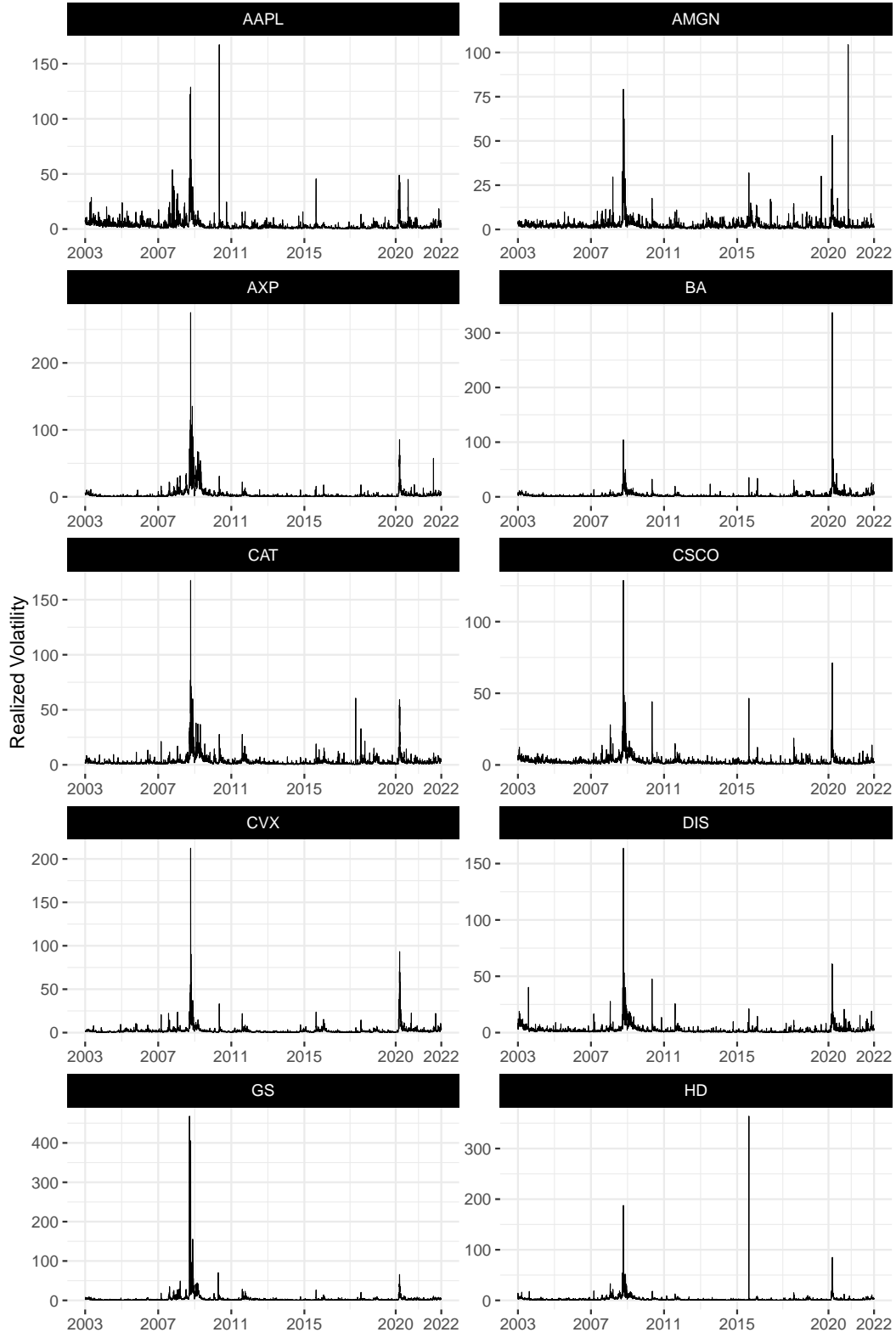


Figure 5: *Daily Realized Variance of individual stocks, January 2, 2003 - June 30, 2022 (4,908 days). Tickers are described in Table 1.*

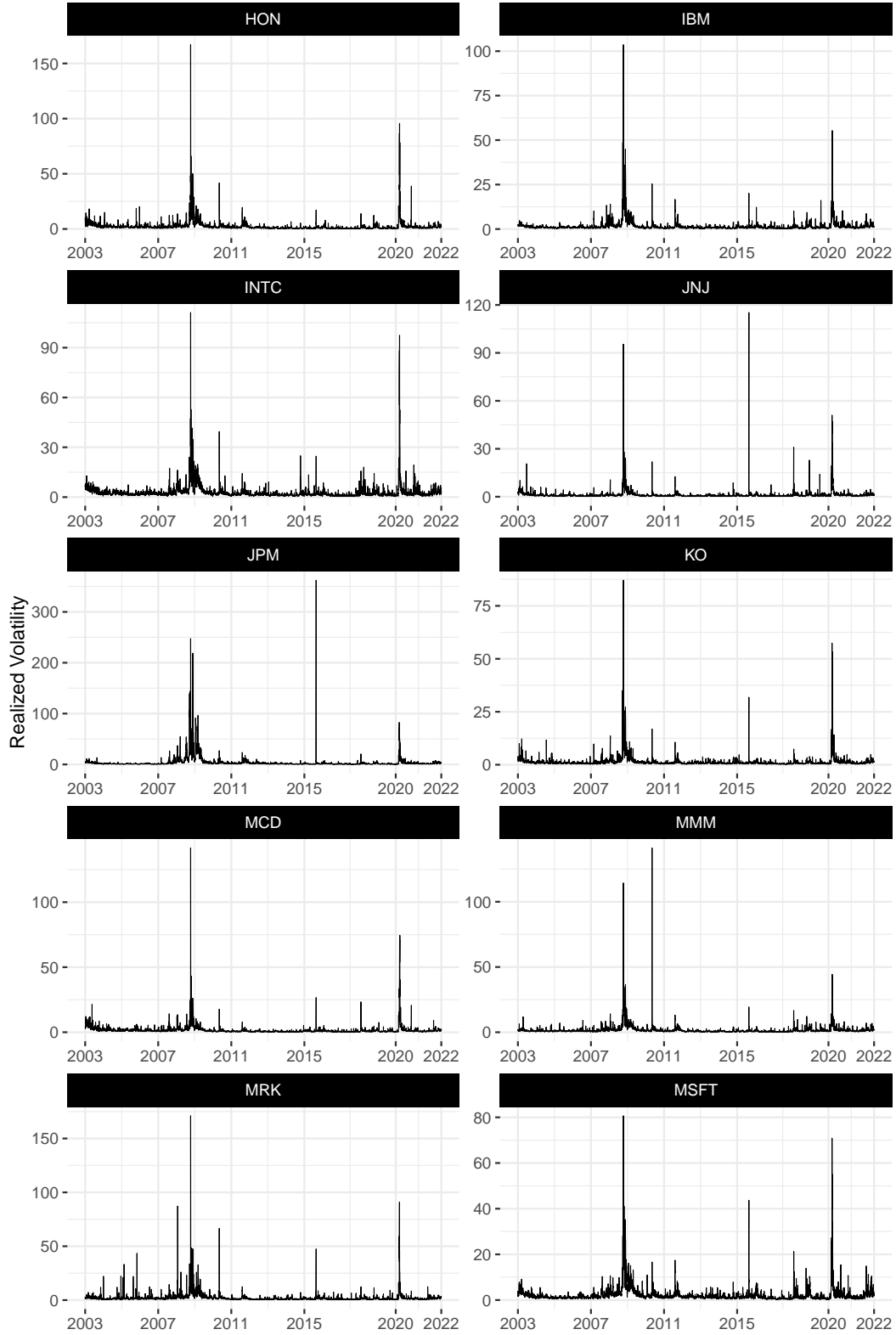


Figure 6: *Daily Realized Variance of individual stocks, January 2, 2003 - June 30, 2022 (4,908 days). Tickers are described in Table 1.*

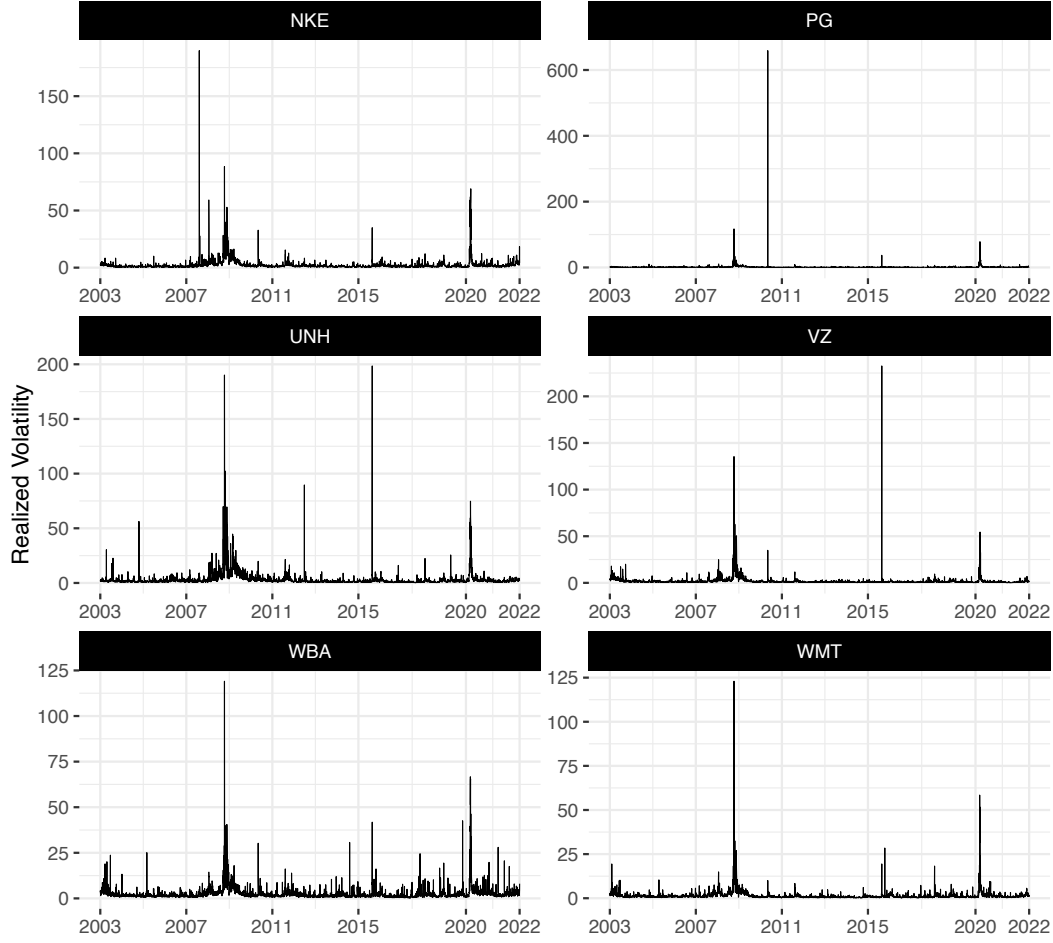


Figure 7: *Daily Realized Variance of individual stocks, January 2, 2003 - June 30, 2022 (4,908 days). Tickers are described in Table 1.*

A2: Alternative hierarchical/grouped representations of different intraday decompositions of daily RV

In Table 2 are reported the eleven hierarchies/groupings deriving from different Temporal-and-Volatility based decompositions. A complete hierarchy/grouping involves the bottom level series produced by a decomposition according to time and/or volatility, and the series forming at least one upper level (by time, quantile or both). A simple hierarchy consists of the top-level series (daily RV) and a single level of bottom time series disaggregated according to time, quantile, or both. The largest decomposition, CTPV(3), involves 24 series, i.e. daily

RV , 3 series distinguished only by quantile thresholds, 5 temporally aggregated series over nonoverlapping, consecutive 78 minutes intervals, 15 series cross-classified by quantile and temporal intervals. This is a grouped series, formed by hierarchies PV(3)-T (see figure 15) and T-PV(3) (see figure 16), whose matrix structural representation is given by figure 27). Instead, the simplest hierarchy, SSV, considers the daily RV as top-level series and two bottom series corresponding to ‘Bad’ ($r_{i,t} < 0$) and ‘Good’ ($r_{i,t} > 0$) volatility, respectively.

Table 2: *Temporal-and-Volatility based intraday RV decompositions*

Name	Intraday decomposition	H/G	n_b	n_a	n	Fig. #	Eq. #
ST	Simple Temporal	H	5	1	6	8	17
SSV	Simple SV (Good & Bad)	H	2	1	3	9	18
STSV	Simple Temporal-and-SV	H	10	1	11	10	19
SV-T	SV with Temporal	H	10	3	13	11	20
T-SV	Temporal with SV	H	10	6	16	12	21
CTSV	Complete Temporal-and-SV	G	10	8	18	—	22
SPV(3)	Simple PV(3)	H	3	1	4	13	23
STPV(3)	Simple Temporal-and-PV(3)	H	15	1	16	14	24
PV(3)-T	PV(3) with Temporal	H	15	4	19	15	25
T-PV(3)	Temporal with PV(3)	H	15	6	21	16	26
CTPV(3)	Complete Temporal-and-PV(3)	G	15	9	24	—	27

H: hierarchy; G: grouping.

n_b : n. of bottom variables; n_a : n. of upper variables; $n = n_b + n_a$.

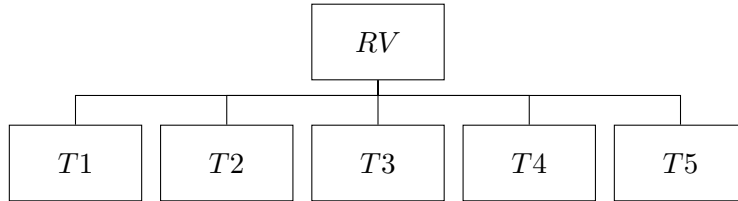


Figure 8: *Hierarchical representation of the Simple Temporal (ST) decomposition of daily RV using five intraday intervals. $n_b = 5, n_a = 1, n = 6$. More details are in Table 2.*

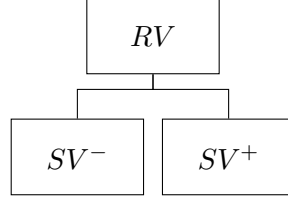


Figure 9: Hierarchical representation of the Simple SV (SSV) decomposition of daily RV . $n_b = 2$, $n_a = 1$, $n = 3$. More details are in Table 2.

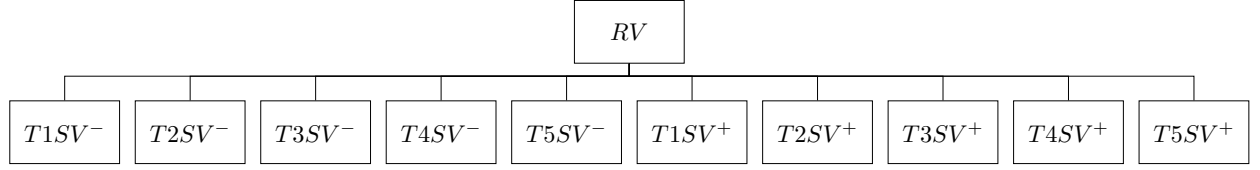


Figure 10: Hierarchical representation of the Simple Temporal-and-SV (STSV) decomposition of daily RV . $n_b = 10$, $n_a = 1$, $n = 11$. More details are in Table 2.

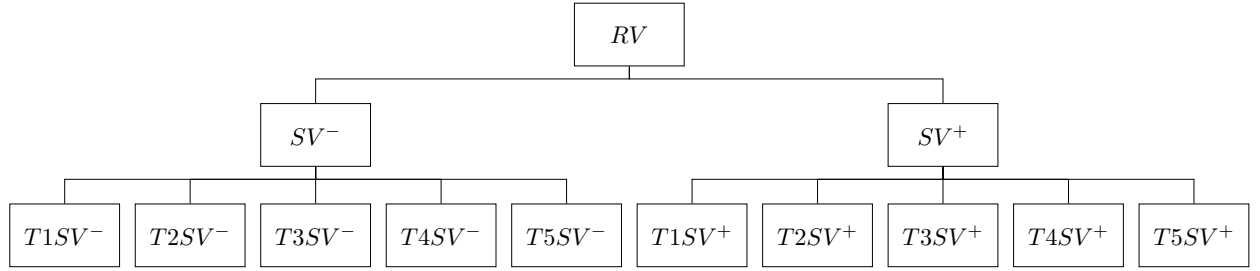


Figure 11: Hierarchical representation of the SV with Temporal (SV-T) decomposition of daily RV . $n_b = 10$, $n_a = 3$, $n = 13$. More details are in Table 2.

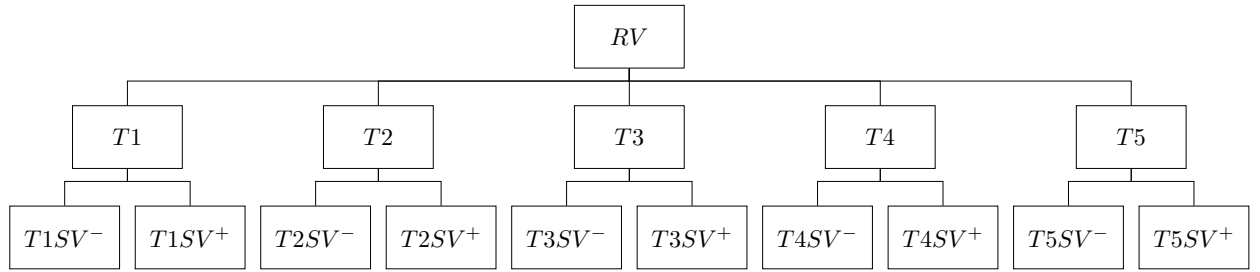


Figure 12: Hierarchical representation of the Temporal with SV (T-SV) decomposition of daily RV . $n_b = 10$, $n_a = 6$, $n = 16$. More details are in Table 2.

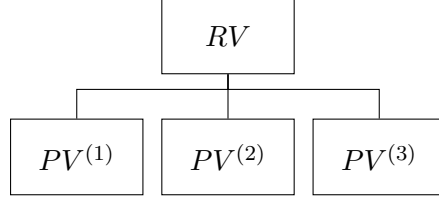


Figure 13: *Hierarchical representation of the Simple $PV(3)$ ($SPV(3)$) decomposition of daily RV . $n_b = 3$, $n_a = 1$, $n = 4$. More details in Table 2.*

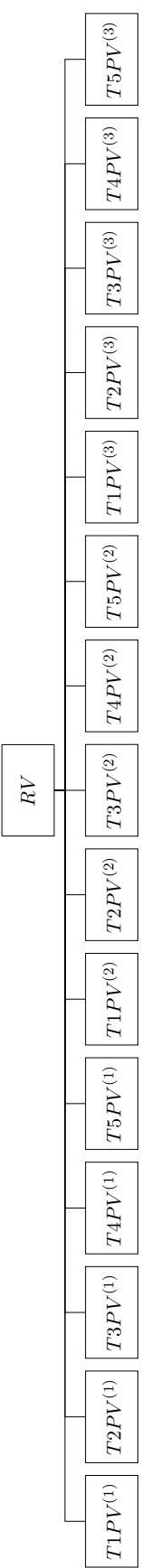


Figure 14: Hierarchical representation of the Simple Temporal-and-PV(3) (STPV(3)) decomposition of daily RV. $n_b = 15$, $n_a = 1$, $n = 16$. More details in Table 2.

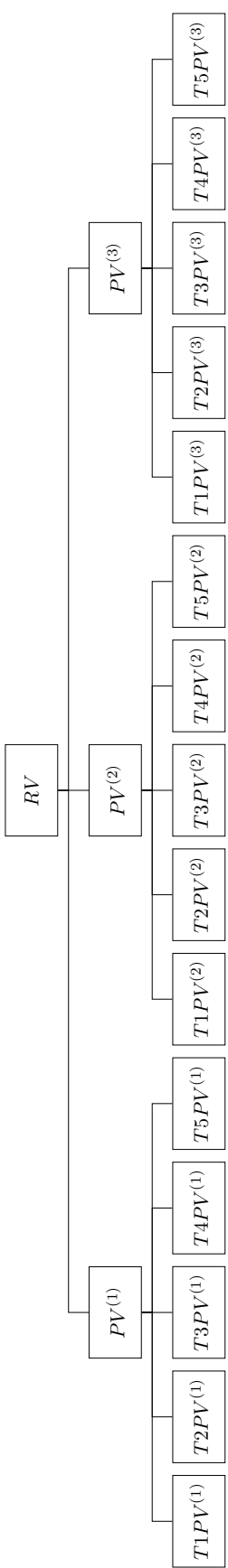


Figure 15: Hierarchical representation of the PV(3) with Temporal (PV(3)-T) decomposition of daily RV. $n_b = 15$, $n_a = 4$, $n = 19$. More details in Table 2.

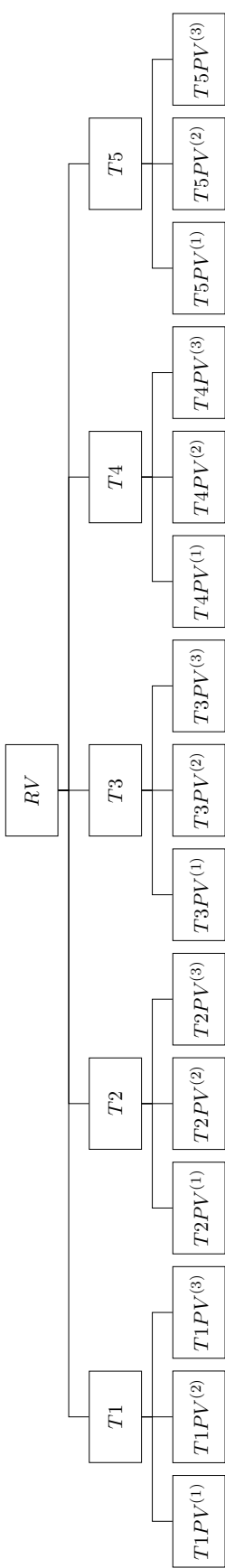


Figure 16: Hierarchical representation of the Temporal with PV(3) (T-PV(3)) decomposition of daily RV. $n_b = 15$, $n_a = 6$, $n = 21$. More details in Table 2.

A3. Structural representations of hierarchies and groupings for different intraday decompositions of daily RV

$$\begin{bmatrix} RV \\ T1 \\ T2 \\ T3 \\ T4 \\ T5 \end{bmatrix} = \begin{bmatrix} \frac{1 \ 1 \ 1 \ 1 \ 1}{\mathbf{I}_5} \end{bmatrix} \begin{bmatrix} T1 \\ T2 \\ T3 \\ T4 \\ T5 \end{bmatrix}$$

Figure 17: Structural representation of the Simple Temporal (ST) decomposition of daily RV using five intraday intervals. $n_b = 5$, $n_a = 1$, $n = 6$.

$$\begin{bmatrix} RV \\ SV^- \\ SV^+ \end{bmatrix} = \begin{bmatrix} \frac{1 \ 1}{\mathbf{I}_2} \end{bmatrix} \begin{bmatrix} SV^- \\ SV^+ \end{bmatrix}$$

Figure 18: Structural representation of the Simple SV (SSV) decomposition of daily RV. $n_b = 2$, $n_a = 1$, $n = 3$.

$$\begin{bmatrix} RV \\ T1SV^- \\ T2SV^- \\ T3SV^- \\ T4SV^- \\ T5SV^- \\ T1SV^+ \\ T2SV^+ \\ T3SV^+ \\ T4SV^+ \\ T5SV^+ \end{bmatrix} = \begin{bmatrix} \frac{1 \ 1 \ 1 \ 1 \ 1 \ 1 \ 1 \ 1 \ 1 \ 1 \ 1}{\mathbf{I}_{10}} \end{bmatrix} \begin{bmatrix} T1SV^- \\ T2SV^- \\ T3SV^- \\ T4SV^- \\ T5SV^- \\ T1SV^+ \\ T2SV^+ \\ T3SV^+ \\ T4SV^+ \\ T5SV^+ \end{bmatrix}$$

Figure 19: Structural representation of the Simple Temporal-and-SV (STSV) decomposition of daily RV. $n_b = 10$, $n_a = 1$, $n = 11$.

Figure 20: *Structural representation of the SV with Temporal (SV-T) decomposition of daily RV. $n_b = 10$, $n_a = 3$, $n = 13$.*

Figure 21: *Structural representation of the Temporal with SV (T-SV) decomposition of daily RV. $n_b = 10$, $n_a = 6$, $n = 16$.*

$$\begin{bmatrix} RV \\ SV^- \\ SV^+ \\ T1 \\ T2 \\ T3 \\ T4 \\ T5 \\ \hline T1SV^- \\ T2SV^- \\ T3SV^- \\ T4SV^- \\ T5SV^- \\ T1SV^+ \\ T2SV^+ \\ T3SV^+ \\ T4SV^+ \\ T5SV^+ \end{bmatrix} = \begin{bmatrix} \begin{array}{ccccccccc} 1 & 1 & 1 & 1 & 1 & 1 & 1 & 1 & 1 \\ 1 & 1 & 1 & 1 & 1 & 0 & 0 & 0 & 0 \\ 0 & 0 & 0 & 0 & 0 & 1 & 1 & 1 & 1 \\ 1 & 0 & 0 & 0 & 0 & 1 & 0 & 0 & 0 \\ 0 & 1 & 0 & 0 & 0 & 0 & 1 & 0 & 0 \\ 0 & 0 & 1 & 0 & 0 & 0 & 0 & 1 & 0 \\ 0 & 0 & 0 & 1 & 0 & 0 & 0 & 0 & 1 \\ 0 & 0 & 0 & 0 & 1 & 0 & 0 & 0 & 1 \end{array} \\[6ex] \textbf{I}_{10} \end{bmatrix} \begin{bmatrix} T1SV^- \\ T2SV^- \\ T3SV^- \\ T4SV^- \\ T5SV^- \\ T1SV^+ \\ T2SV^+ \\ T3SV^+ \\ T4SV^+ \\ T5SV^+ \end{bmatrix}$$

Figure 22: *Structural representation of the grouped time series describing the Complete Temporal-and-SV (CTSV) decomposition of daily RV using five intraday intervals and Semi Variances (Bad & Good volatility). $n_b = 10$, $n_a = 8$, $n = 18$. The grouped time series is obtained by merging the hierarchies SV-T and T-SV, described in Figures 11 and 12, respectively.*

$$\begin{bmatrix} RV \\ PV^{(1)} \\ PV^{(2)} \\ PV^{(3)} \end{bmatrix} = \begin{bmatrix} \frac{1}{3} & \frac{1}{3} & \frac{1}{3} \\ \mathbf{I}_3 \end{bmatrix} \begin{bmatrix} PV^{(1)} \\ PV^{(2)} \\ PV^{(3)} \end{bmatrix}$$

Figure 23: Structural representation of the Simple PV(3) (SPV(3)) decomposition of daily RV. $n_b = 3$, $n_a = 1$, $n = 4$.

$$\begin{bmatrix} RV \\ T1PV^{(1)} \\ T2PV^{(1)} \\ T3PV^{(1)} \\ T4PV^{(1)} \\ T5PV^{(1)} \\ T1PV^{(2)} \\ T2PV^{(2)} \\ T3PV^{(2)} \\ T4PV^{(2)} \\ T5PV^{(2)} \\ T1PV^{(3)} \\ T2PV^{(3)} \\ T3PV^{(3)} \\ T4PV^{(3)} \\ T5PV^{(3)} \end{bmatrix} = \begin{bmatrix} \begin{array}{cccccccccccccccc} 1 & 1 & 1 & 1 & 1 & 1 & 1 & 1 & 1 & 1 & 1 & 1 & 1 & 1 & 1 & 1 \end{array} \\ \\ \\ \\ \\ \\ \\ \\ \\ \\ \\ \\ \\ \\ \\ \\ \end{bmatrix} \mathbf{I}_{15} \begin{bmatrix} T1PV^{(1)} \\ T2PV^{(1)} \\ T3PV^{(1)} \\ T4PV^{(1)} \\ T5PV^{(1)} \\ T1PV^{(2)} \\ T2PV^{(2)} \\ T3PV^{(2)} \\ T4PV^{(2)} \\ T5PV^{(2)} \\ T1PV^{(3)} \\ T2PV^{(3)} \\ T3PV^{(3)} \\ T4PV^{(3)} \\ T5PV^{(3)} \end{bmatrix}$$

Figure 24: Structural representation of the Simple Temporal-and-PV(3) (STPV(3)) decomposition of daily RV. $n_b = 15$, $n_a = 1$, $n = 16$.

[illegible]

Figure 25: *Structural representation of the PV(3) with Temporal (PV(3)-T) decomposition of daily RV. $n_b = 15$, $n_a = 4$, $n = 19$.*

$$\begin{bmatrix} RV \\ T1 \\ T2 \\ T3 \\ T4 \\ T5 \\ T1PV^{(1)} \\ T2PV^{(1)} \\ T3PV^{(1)} \\ T4PV^{(1)} \\ T5PV^{(1)} \\ T1PV^{(2)} \\ T2PV^{(2)} \\ T3PV^{(2)} \\ T4PV^{(2)} \\ T5PV^{(2)} \\ T1PV^{(3)} \\ T2PV^{(3)} \\ T3PV^{(3)} \\ T4PV^{(3)} \\ T5PV^{(3)} \end{bmatrix} = \begin{bmatrix} 1 & 1 & 1 & 1 & 1 & 1 & 1 & 1 & 1 & 1 & 1 & 1 & 1 & 1 & 1 & 1 \\ 1 & 0 & 0 & 0 & 0 & 1 & 0 & 0 & 0 & 0 & 1 & 0 & 0 & 0 & 0 & 0 \\ 0 & 1 & 0 & 0 & 0 & 0 & 1 & 0 & 0 & 0 & 0 & 1 & 0 & 0 & 0 & 0 \\ 0 & 0 & 1 & 0 & 0 & 0 & 0 & 1 & 0 & 0 & 0 & 0 & 1 & 0 & 0 & 0 \\ 0 & 0 & 0 & 1 & 0 & 0 & 0 & 0 & 1 & 0 & 0 & 0 & 0 & 1 & 0 & 0 \\ 0 & 0 & 0 & 0 & 1 & 0 & 0 & 0 & 0 & 1 & 0 & 0 & 0 & 0 & 0 & 1 \end{bmatrix}$$

Figure 26: *Structural representation of the Temporal with PV(3) (T-PV(3)) decomposition of daily RV. $n_b = 15$, $n_a = 6$, $n = 21$.*

A4: Forecasting accuracy in different test periods

	2007-2022		2007-2010		2011-2014		2015-2019		2020-2022	
	MSE	QLIKE	MSE	QLIKE	MSE	QLIKE	MSE	QLIKE	MSE	QLIKE
<i>Panel A: DJIA index</i>										
$PV(3)$	0.775	0.816	0.921	0.997	1.059	2.691	2.272	1.073	0.873	6.045
$PV(3)_{bu}$	0.922	0.924	1.036	0.947	0.911	1.023	1.001	1.076	1.004	0.874
$PV(3)_{shr}$	0.812	0.833	0.944	0.934	0.947	0.941	0.945	1.047	0.902	0.902
SV	1.024	1.028	0.991	1.069	1.048	0.978	0.973	0.986	0.968	0.962
SV_{bu}	0.962	0.960	1.055	0.966	0.923	1.024	1.010	1.069	1.021	0.897
SV_{shr}	0.976	0.976	1.022	0.997	0.960	0.997	0.983	1.027	0.989	0.896
$TPV(3)_{bu}$	0.799	0.822	1.148	0.911	0.916	1.092	1.090	1.265	1.075	0.893
$TPV(3)_{shr}$	0.787	0.808	0.992	0.900	0.915	0.967	0.971	1.095	0.944	0.874
TSV_{bu}	0.801	0.824	1.151	0.914	0.923	1.085	1.085	1.245	1.074	0.906
TSV_{shr}	0.856	0.869	1.066	0.930	0.923	1.020	1.011	1.109	1.011	0.873
<i>Panel B: Individual stocks</i>										
$PV(3)$	0.938	0.899	0.973	0.836	1.097	1.421	1.364	1.046	1.344	1.035
$PV(3)_{bu}$	0.953	0.943	0.993	0.950	0.994	1.003	0.900	1.010	0.990	0.709
$PV(3)_{shr}$	0.916	0.896	0.927	0.874	1.030	0.939	0.833	0.970	0.898	0.704
SV	0.993	1.016	1.022	1.005	1.073	1.124	1.092	1.076	1.080	0.963
SV_{bu}	0.967	0.964	1.000	0.973	0.998	1.000	0.921	1.007	1.006	0.779
SV_{shr}	0.970	0.980	0.985	0.979	1.029	0.992	0.899	0.988	0.987	0.742
$TPV(3)_{bu}$	1.027	0.982	1.063	0.859	1.011	1.029	0.894	1.134	1.030	0.641
$TPV(3)_{shr}$	0.963	0.924	0.963	0.848	0.991	0.923	0.805	1.013	0.918	0.606
TSV_{bu}	1.028	0.991	1.060	0.867	1.023	1.019	0.893	1.119	1.029	0.656
TSV_{shr}	1.009	0.987	1.014	0.907	0.997	0.959	0.850	1.041	0.991	0.632

Table 3: Accuracy of the *one-day ahead* forecasts. MSE and QLIKE ratios for the DJIA index (panel A), and geometric means of the MSE and QLIKE ratios for individual stocks (panel B) over the benchmark HAR model. Values larger than one in red. The best index value in each column is highlighted in bold.

	2007-2022		2007-2010		2011-2014		2015-2019		2020-2022	
	MSE	QLIKE	MSE	QLIKE	MSE	QLIKE	MSE	QLIKE	MSE	QLIKE
<i>Panel A: DJIA index</i>										
$PV(3)$	1.047	1.077	0.973	1.013	1.163	1.645	0.977	1.021	0.908	0.942
$PV(3)_{bu}$	0.981	0.957	1.013	0.979	0.892	1.015	0.235	1.058	1.011	0.049
$PV(3)_{shr}$	1.010	1.015	0.963	0.975	1.033	0.946	0.225	1.030	0.938	0.051
SV	1.012	1.017	1.011	0.999	1.030	0.985	0.997	0.988	0.986	1.000
SV_{bu}	0.991	0.972	1.016	0.985	0.921	1.014	0.237	1.049	1.021	0.051
SV_{shr}	0.998	0.991	1.006	0.983	0.975	0.995	0.233	1.020	0.995	0.053
$TPV(3)_{bu}$	0.766	0.795	1.078	0.978	0.832	1.067	0.250	1.231	1.049	0.051
$TPV(3)_{shr}$	0.909	0.925	0.984	0.962	0.956	0.956	0.227	1.061	0.948	0.050
TSV_{bu}	0.774	0.801	1.072	0.977	0.833	1.063	0.249	1.210	1.045	0.051
TSV_{shr}	0.853	0.878	1.031	0.967	0.920	1.009	0.236	1.094	0.999	0.050
<i>Panel B: Individual stocks</i>										
$PV(3)$	1.035	0.976	0.958	0.943	0.978	1.139	1.025	0.955	1.029	0.865
$PV(3)_{bu}$	0.981	0.982	0.999	0.984	0.990	1.010	0.895	1.013	0.984	0.750
$PV(3)_{shr}$	0.998	0.964	0.955	0.949	0.971	0.956	0.824	0.965	0.929	0.662
SV	1.014	1.008	0.985	1.001	1.005	1.004	0.998	0.982	0.993	1.025
SV_{bu}	0.991	0.992	1.001	0.991	1.000	1.010	0.977	1.008	0.999	0.946
SV_{shr}	0.998	0.996	0.987	0.992	1.000	1.001	0.947	0.991	0.990	0.897
$TPV(3)_{bu}$	0.996	1.039	1.055	0.994	1.000	1.083	0.902	1.123	0.993	0.655
$TPV(3)_{shr}$	0.973	0.967	0.972	0.955	0.965	0.963	0.793	0.990	0.924	0.565
TSV_{bu}	1.004	1.054	1.048	0.994	1.021	1.076	0.908	1.108	0.994	0.698
TSV_{shr}	0.987	1.007	1.010	0.987	0.988	1.018	0.861	1.043	0.979	0.646

Table 4: Accuracy of the *five-day ahead* forecasts. MSE and QLIKE ratios for the DJIA index (panel A), and geometric means of the MSE and QLIKE ratios for individual stocks (panel B) over the benchmark HAR model. Values larger than one in red. The best index value in each column is highlighted in bold.

	2007-2022		2007-2010		2011-2014		2015-2019		2020-2022	
	MSE	QLIKE	MSE	QLIKE	MSE	QLIKE	MSE	QLIKE	MSE	QLIKE
<i>Panel A: DJIA index</i>										
$PV(3)$	1.030	1.025	1.001	0.988	1.012	0.995	0.962	1.011	0.969	0.954
$PV(3)_{bu}$	1.010	1.009	1.009	0.988	1.006	1.011	0.596	1.021	1.000	0.460
$PV(3)_{shr}$	1.018	1.015	1.003	0.983	1.005	1.000	0.596	1.015	0.976	0.465
SV	1.002	1.003	0.998	1.003	1.006	1.001	0.928	0.999	0.996	0.904
SV_{bu}	1.007	1.005	1.007	0.991	1.003	1.011	0.748	1.014	1.004	0.662
SV_{shr}	1.002	1.002	1.003	1.000	1.003	1.006	0.728	1.007	0.996	0.637
$TPV(3)_{bu}$	1.125	1.103	1.064	0.991	1.037	1.054	0.386	1.106	1.007	0.169
$TPV(3)_{shr}$	0.914	0.939	1.057	0.989	1.012	0.997	0.374	1.032	0.977	0.169
TSV_{bu}	1.121	1.099	1.055	0.991	1.035	1.047	0.385	1.092	1.006	0.170
TSV_{shr}	0.949	0.965	1.044	1.005	1.010	1.014	0.379	1.053	0.997	0.169
<i>Panel B: Individual stocks</i>										
$PV(3)$	1.049	1.010	0.990	0.941	0.964	0.980	1.055	0.976	1.016	1.106
$PV(3)_{bu}$	0.997	0.995	1.004	0.980	0.997	1.009	0.945	1.008	0.982	0.899
$PV(3)_{shr}$	1.017	0.994	0.993	0.949	0.970	0.983	0.916	0.988	0.961	0.865
SV	1.001	1.001	0.990	1.005	1.001	1.000	0.993	0.988	0.997	0.994
SV_{bu}	0.998	0.998	1.001	0.992	1.001	1.008	0.971	1.003	0.995	0.942
SV_{shr}	0.997	0.998	0.993	0.995	1.000	1.003	0.960	0.995	0.993	0.927
$TPV(3)_{bu}$	1.038	1.012	1.053	0.955	1.000	1.058	0.868	1.065	0.978	0.712
$TPV(3)_{shr}$	0.982	0.965	1.013	0.941	0.960	0.989	0.824	0.996	0.956	0.672
TSV_{bu}	1.043	1.019	1.043	0.960	1.006	1.051	0.875	1.055	0.980	0.730
TSV_{shr}	0.994	0.984	1.018	0.971	0.990	1.016	0.853	1.023	0.979	0.706

Table 5: Accuracy of the **22-day ahead** forecasts. MSE and QLIKE ratios for the DJIA index (panel A), and geometric means of the MSE and QLIKE ratios for individual stocks (panel B) over the benchmark HAR model. Values larger than one in red. The best index value in each column is highlighted in bold.

	<i>RV</i>	<i>SV</i>	<i>PV(3)</i>	<i>SV_{bu}</i>	<i>TSV_{bu}</i>	<i>PV(3)_{bu}</i>	<i>TPV(3)_{bu}</i>	<i>SV_{shr}</i>	<i>TSV_{shr}</i>	<i>PV(3)_{shr}</i>	<i>TPV(3)_{shr}</i>
<i>Panel A: DJIA index</i>											
<i>MSE</i>	6.352	6.527	5.184	6.099	5.236	5.867	5.219	6.202	5.523	5.293	5.135
<i>p-value dm_{RV}</i>	—	0.785	0.168	0.142	0.119	0.075	0.121	0.119	0.118	0.066	0.074
<i>p-value dm_{SV}</i>	—	—	0.131	0.148	0.112	0.079	0.114	0.115	0.110	0.044	0.064
<i>p-value dm_{PV}</i>	—	—	—	0.800	0.526	0.759	0.517	0.821	0.659	0.579	0.467
<i>p-value MCS</i>	0.412	0.299	0.687	0.535	0.559	0.605	0.657	0.496	0.572	0.804	1.000
<i>QLIKE</i>	0.216	0.210	0.491	0.218	0.235	0.217	0.236	0.212	0.219	0.204	0.210
<i>p-value dm_{RV}</i>	—	0.004	0.908	0.692	1.000	0.528	1.000	0.176	0.698	0.008	0.104
<i>p-value dm_{SV}</i>	—	—	0.911	0.988	1.000	0.956	1.000	0.796	0.997	0.031	0.452
<i>p-value dm_{PV}</i>	—	—	—	0.098	0.112	0.097	0.113	0.093	0.098	0.087	0.092
<i>p-value MCS</i>	0.279	0.119	0.231	0.029	0.000	0.117	0.000	0.061	0.015	1.000	0.361
<i>Panel B: Individual stocks</i>											
<i>MSE</i>	39.595	40.993	36.374	37.805	58.265	36.947	55.191	38.970	45.080	35.553	37.942
<i>p-value dm_{RV}</i>	—	0	0	1	0	2	0	1	2	2	8
<i>p-value dm_{SV}</i>	—	—	0	0	1	1	1	5	3	2	8
<i>p-value dm_{PV}</i>	—	—	—	1	0	1	0	2	1	1	2
<i>p-value MCS</i>	25	23	26	25	23	24	25	23	25	26	26
<i>QLIKE</i>	0.185	0.214	0.269	0.170	0.161	0.165	0.161	0.165	0.154	0.151	0.145
<i>p-value dm_{RV}</i>	—	2	1	2	4	4	4	7	6	19	16
<i>p-value dm_{SV}</i>	—	—	1	6	5	7	5	10	7	20	17
<i>p-value dm_{PV}</i>	—	—	—	7	7	8	7	8	8	10	8
<i>p-value MCS</i>	14	14	18	8	4	6	6	10	4	26	13

Note: The table reports the **one-step ahead** forecasting performance of the different models. The top panel shows the results for the DJIA index. Diebold-Mariano: p -values < 0.05 are highlighted in bold. MCS: p -values > 0.2 are highlighted in bold. The bottom panel reports the average loss and 5% rejection frequency of the Diebold-Mariano tests for each individual stocks. The one-sided tests between each forecasting model against HAR , SV , and $PV(3)$ are denoted by dm_{HAR} , dm_{SV} , and $dm_{PV(3)}$, respectively. MCS denotes the p -value of that model being in the Model Confidence Set, or the number of times that model is in the 80% Model Confidence Set. $PV(3)$ denotes the $HAR - PV(3)$ model with 3 decompositions defined by two thresholds at 10% and 75%.

Table 6: *One-day-ahead forecasting performance: 2007-2022 (3,901 days)*

	RV	SV	$PV(3)$	SV_{bu}	TSV_{bu}	$PV(3)_{bu}$	$TPV(3)_{bu}$	SV_{shr}	TSV_{shr}	$PV(3)_{shr}$	$TPV(3)_{shr}$
<i>Panel A: DJIA index</i>											
<i>MSE</i>	5.109	5.195	5.503	4.966	4.093	4.888	4.064	5.064	4.487	5.185	4.724
p -value dm_{RV}	—	0.774	0.833	0.021	0.002	0.007	0.002	0.235	0.000	0.613	0.041
p -value dm_{SV}	—	—	0.783	0.054	0.002	0.023	0.002	0.049	0.000	0.485	0.023
p -value dm_{PV}	—	—	—	0.105	0.010	0.077	0.009	0.139	0.018	0.027	0.003
p -value MCS	0.194	0.194	0.203	0.329	0.308	0.313	1.000	0.227	0.226	0.234	0.358
<i>QLIKE</i>	0.930	0.927	0.908	0.220	0.231	0.219	0.233	0.217	0.219	0.209	0.211
p -value dm_{RV}	—	0.000	0.441	0.008	0.009	0.008	0.009	0.008	0.008	0.007	0.007
p -value dm_{SV}	—	—	0.449	0.008	0.009	0.008	0.009	0.008	0.008	0.007	0.007
p -value dm_{PV}	—	—	—	0.007	0.008	0.007	0.008	0.007	0.007	0.006	0.006
p -value MCS	0.496	0.497	0.165	0.008	0.000	0.054	0.000	0.039	0.006	1.000	0.218
<i>Panel B: Individual stocks</i>											
<i>MSE</i>	25.109	25.371	22.936	24.804	28.938	24.433	28.072	24.923	25.730	22.753	23.185
p -value dm_{RV}	—	0	1	2	3	9	4	4	5	2	7
p -value dm_{SV}	—	—	1	2	4	4	5	4	7	3	5
p -value dm_{PV}	—	—	—	0	0	0	0	0	0	0	1
p -value MCS	25	25	26	25	22	26	26	25	26	26	26
<i>QLIKE</i>	0.186	0.187	0.201	0.181	0.162	0.161	0.161	0.174	0.153	0.147	0.141
p -value dm_{RV}	—	6	7	4	5	8	6	9	8	24	22
p -value dm_{SV}	—	—	7	2	3	4	4	3	5	21	19
p -value dm_{PV}	—	—	—	2	4	4	4	2	6	8	10
p -value MCS	11	13	22	11	6	9	7	11	7	23	22

Note: The table reports the **five-step ahead** forecasting performance of the different models. The top panel shows the results for the DJIA index. Diebold-Mariano: p -values < 0.05 are highlighted in bold. MCS: p -values > 0.2 are highlighted in bold. The bottom panel reports the average loss and 5% rejection frequency of the Diebold-Mariano tests for each individual stocks. The one-sided tests between each forecasting model against HAR , SV , and $PV(3)$ are denoted by dm_{HAR} , dm_{SV} , and $dm_{PV(3)}$, respectively. MCS denotes the p -value of that model being in the Model Confidence Set, or the number of times that model is in the 80% Model Confidence Set. $PV(3)$ denotes the $HAR - PV(3)$ model with 3 decompositions defined by two thresholds at 10% and 75%.

Table 7: Five-day-ahead forecasting performance: 2007-2022 (3,897 days)

	RV	SV	$PV(3)$	SV_{bu}	TSV_{bu}	$PV(3)_{bu}$	$TPV(3)_{bu}$	SV_{shr}	TSV_{shr}	$PV(3)_{shr}$	$TPV(3)_{shr}$
<i>Panel A: DJIA index</i>											
<i>MSE</i>	4.424	4.436	4.533	4.448	4.861	4.463	4.879	4.434	4.267	4.488	4.153
p -value dm_{RV}	—	0.613	0.851	0.631	0.947	0.683	0.956	0.569	0.122	0.780	0.034
p -value dm_{SV}	—	—	0.843	0.575	0.948	0.646	0.956	0.478	0.079	0.765	0.016
p -value dm_{PV}	—	—	—	0.209	0.890	0.257	0.904	0.158	0.030	0.225	0.005
p -value MCS	0.332	0.272	0.478	0.336	0.689	0.342	0.632	0.314	0.127	0.475	1.000
<i>QLIKE</i>	0.973	0.902	0.936	0.727	0.375	0.580	0.376	0.708	0.368	0.580	0.364
p -value dm_{RV}	—	0.160	0.150	0.027	0.000	0.002	0.000	0.016	0.000	0.002	0.000
p -value dm_{SV}	—	—	0.830	0.049	0.000	0.004	0.000	0.028	0.000	0.003	0.000
p -value dm_{PV}	—	—	—	0.031	0.000	0.002	0.000	0.017	0.000	0.002	0.000
p -value MCS	0.450	0.431	0.396	0.378	0.079	0.379	0.100	0.380	0.001	0.378	1.000
<i>Panel B: Individual stocks</i>											
<i>MSE</i>	14.243	14.277	14.316	14.205	14.011	14.231	13.905	14.207	13.567	14.122	13.257
p -value dm_{RV}	—	1	2	2	2	4	3	3	5	3	11
p -value dm_{SV}	—	—	2	1	2	2	3	2	5	2	11
p -value dm_{PV}	—	—	—	3	1	2	1	3	1	6	12
p -value MCS	25	26	26	24	23	26	23	25	24	23	25
<i>QLIKE</i>	0.269	0.268	0.292	0.262	0.227	0.255	0.225	0.259	0.222	0.247	0.214
p -value dm_{RV}	—	5	6	4	12	10	12	6	13	22	22
p -value dm_{SV}	—	—	5	3	10	6	10	4	13	17	20
p -value dm_{PV}	—	—	—	8	14	10	14	9	15	14	15
p -value MCS	16	19	23	15	7	19	9	17	7	24	25

Note: The table reports the **22-step ahead** forecasting performance of the different models. The top panel shows the results for the DJIA index. Diebold-Mariano: p -values < 0.05 are highlighted in bold. MCS: p -values > 0.2 are highlighted in bold. The bottom panel reports the average loss and 5% rejection frequency of the Diebold-Mariano tests for each individual stocks. The one-sided tests between each forecasting model against HAR , SV , and $PV(3)$ are denoted by dm_{HAR} , dm_{SV} , and $dm_{PV(3)}$, respectively. MCS denotes the p -value of that model being in the Model Confidence Set, or the number of times that model is in the 80% Model Confidence Set. $PV(3)$ denotes the $HAR - PV(3)$ model with 3 decompositions defined by two thresholds at 10% and 75%.

Table 8: *Twenty-two-day-ahead forecasting performance: 2007-2022 (3,880 days)*

	RV	SV	$PV(3)$	SV_{bu}	TSV_{bu}	$PV(3)_{bu}$	$TPV(3)_{bu}$	SV_{shr}	TSV_{shr}	$PV(3)_{shr}$	$TPV(3)_{shr}$
<i>Panel A: DJIA index</i>											
MSE	20.587	21.074	15.957	19.808	16.485	18.972	16.440	20.097	17.614	16.718	16.198
p -value dm_{RV}	—	0.718	0.162	0.197	0.131	0.107	0.134	0.159	0.136	0.077	0.089
p -value dm_{SV}	—	—	0.135	0.211	0.132	0.121	0.134	0.174	0.137	0.060	0.084
p -value dm_{PV}	—	—	—	0.820	0.567	0.789	0.560	0.833	0.697	0.639	0.541
p -value MCS	0.546	0.472	1.000	0.468	0.385	0.581	0.382	0.534	0.468	0.686	0.490
$QLIKE$	0.187	0.183	0.505	0.192	0.203	0.192	0.205	0.187	0.191	0.176	0.181
p -value dm_{RV}	—	0.002	0.873	0.999	1.000	0.996	1.000	0.267	0.995	0.001	0.016
p -value dm_{SV}	—	—	0.876	1.000	1.000	1.000	1.000	0.999	1.000	0.024	0.231
p -value dm_{PV}	—	—	—	0.131	0.140	0.131	0.141	0.127	0.130	0.119	0.123
p -value MCS	0.020	0.269	0.193	0.000	0.000	0.000	0.000	0.022	0.000	1.000	0.000
<i>Panel B: Individual stocks</i>											
MSE	96.815	97.020	95.505	93.645	186.003	92.522	175.154	94.130	130.389	91.192	107.195
p -value dm_{RV}	—	0	0	0	0	2	0	0	0	3	5
p -value dm_{SV}	—	—	0	1	1	1	1	2	1	3	4
p -value dm_{PV}	—	—	—	1	0	1	0	1	0	1	1
p -value MCS	26	24	26	23	25	25	24	26	25	26	26
$QLIKE$	0.196	0.224	0.287	0.188	0.171	0.191	0.172	0.187	0.163	0.166	0.156
p -value dm_{RV}	—	4	0	0	1	1	1	3	1	13	9
p -value dm_{SV}	—	—	1	1	0	0	0	3	0	9	5
p -value dm_{PV}	—	—	—	4	2	3	2	5	3	6	3
p -value MCS	15	18	21	10	1	12	3	15	5	26	13

Note: The table reports **the one-step ahead** forecasting performance of the different models. The top panel shows the results for the DJIA index.

Diebold-Mariano: p -values < 0.05 are highlighted in bold. The bottom panel reports the average loss and 5% rejection frequency of the

Diebold-Mariano tests for each individual stocks. The one-sided tests between each forecasting model against HAR , SV , and $PV(3)$ models are denoted by dm_{HAR} , dm_{SV} , and $dm_{PV(3)}$, respectively. MCS denotes the p -value of that model being in the Model Confidence Set, or the number of times that model is in the 80% Model Confidence Set. $PV(3)$ denotes the HAR-PV(3) model with 3 decompositions defined by two thresholds at 10% and 75%.

Table 9: Forecasting performance: 2007-2010 (1,008 days).

	RV	SV	PV(3)	SV _{bu}	TSV _{bu}	PV(3) _{bu}	TPV(3) _{bu}	SV _{shr}	TSV _{shr}	PV(3) _{shr}	TPV(3) _{shr}
<i>Panel A: DJIA index</i>											
<i>MSE</i>	0.433	0.429	0.399	0.457	0.498	0.449	0.497	0.442	0.462	0.409	0.429
<i>p</i> -value dm_{RV}	—	0.339	0.242	0.991	0.997	0.942	0.997	0.995	0.985	0.100	0.389
<i>p</i> -value dm_{SV}	—	—	0.266	0.929	0.989	0.849	0.990	0.866	0.951	0.184	0.506
<i>p</i> -value dm_{PV}	—	—	—	0.860	0.940	0.834	0.940	0.803	0.867	0.621	0.769
<i>p</i> -value MCS	0.465	0.633	1.000	0.123	0.113	0.101	0.101	0.281	0.165	0.668	0.259
<i>QLIKE</i>	0.195	0.192	0.209	0.209	0.243	0.210	0.247	0.200	0.216	0.204	0.214
<i>p</i> -value dm_{RV}	—	0.003	1.000	1.000	1.000	1.000	1.000	1.000	1.000	1.000	1.000
<i>p</i> -value dm_{SV}	—	—	1.000	1.000	1.000	1.000	1.000	1.000	1.000	1.000	1.000
<i>p</i> -value dm_{PV}	—	—	—	0.423	1.000	0.555	1.000	0.014	0.948	0.025	0.914
<i>p</i> -value MCS	0.009	1.000	0.036	0.009	0.000	0.001	0.000	0.000	0.000	0.027	0.000
<i>Panel B: Individual stocks</i>											
<i>MSE</i>	1.508	1.568	1.464	1.504	1.564	1.492	1.569	1.494	1.514	1.404	1.445
<i>p</i> -value dm_{RV}	—	1	4	3	1	5	1	7	2	9	6
<i>p</i> -value dm_{SV}	—	—	3	1	1	1	1	4	0	10	4
<i>p</i> -value dm_{PV}	—	—	—	0	0	0	0	0	0	2	1
<i>p</i> -value MCS	22	20	25	21	8	21	11	21	11	24	13
<i>QLIKE</i>	0.123	0.148	0.133	0.124	0.134	0.124	0.136	0.121	0.126	0.118	0.123
<i>p</i> -value dm_{RV}	—	8	4	1	1	1	1	10	2	14	3
<i>p</i> -value dm_{SV}	—	—	5	3	1	3	1	5	1	9	2
<i>p</i> -value dm_{PV}	—	—	—	6	2	6	2	9	5	14	6
<i>p</i> -value MCS	15	16	17	9	0	8	1	15	1	21	6

Note: The table reports the **one-step ahead** forecasting performance of the different models. The top panel shows the results for the DJIA index.

Diebold-Mariano *p*-values < 0.05 are highlighted in bold. The bottom panel reports the average loss and 5% rejection frequency of the Diebold-Mariano tests for each individual stocks. The one-sided tests between each forecasting model against RV-HAR, SV-HAR, and PV(3)-HAR are denoted by dm_{HAR} , dm_{SV} , and $dm_{PV(3)}$, respectively. MCS denotes the *p*-value of that model being in the Model Confidence Set, or the number of times that model is in the 80% Model Confidence Set. PV(3) denotes the HAR-PV(3) model with 3 decompositions defined by two thresholds at 10% and 75%.

Table 10: Forecasting performance: 2011-2014 (1,006 days).

	<i>RV</i>	<i>SV</i>	<i>PV(3)</i>	<i>SV_{bu}</i>	<i>TSV_{bu}</i>	<i>PV(3)_{bu}</i>	<i>TPV(3)_{bu}</i>	<i>SV_{shr}</i>	<i>TSV_{shr}</i>	<i>PV(3)_{shr}</i>	<i>TPV(3)_{shr}</i>
<i>Panel A: DJIA index</i>											
<i>MSE</i>	0.901	0.963	0.899	0.871	0.824	0.854	0.822	0.898	0.839	0.841	0.811
<i>p</i> -value <i>dm_{RV}</i>	—	0.830	0.485	0.145	0.093	0.113	0.091	0.384	0.062	0.103	0.050
<i>p</i> -value <i>dm_{SV}</i>	—	—	0.294	0.155	0.122	0.141	0.121	0.139	0.106	0.124	0.090
<i>p</i> -value <i>dm_{PV}</i>	—	—	—	0.324	0.124	0.216	0.114	0.498	0.164	0.056	0.038
<i>p</i> -value MCS	0.606	0.545	0.560	0.617	0.290	0.349	0.220	0.592	0.830	0.620	1.000
<i>QLIKE</i>	0.242	0.234	0.211	0.247	0.260	0.243	0.260	0.239	0.245	0.218	0.228
<i>p</i> -value <i>dm_{RV}</i>	—	0.012	0.008	0.866	0.997	0.597	0.999	0.023	0.956	0.001	0.010
<i>p</i> -value <i>dm_{SV}</i>	—	—	0.024	0.951	0.996	0.893	0.998	0.977	0.998	0.006	0.112
<i>p</i> -value <i>dm_{PV}</i>	—	—	—	0.987	0.998	0.984	0.999	0.986	0.996	0.875	0.985
<i>p</i> -value MCS	0.024	0.037	1.000	0.053	0.008	0.089	0.003	0.062	0.003	0.230	0.034
<i>Panel B: Individual stocks</i>											
<i>MSE</i>	28.790	28.277	13.400	25.753	16.027	24.144	15.524	26.345	19.594	17.863	16.205
<i>p</i> -value <i>dm_{RV}</i>	—	2	1	0	1	3	2	4	0	9	12
<i>p</i> -value <i>dm_{SV}</i>	—	—	3	1	0	1	1	2	1	7	9
<i>p</i> -value <i>dm_{PV}</i>	—	—	—	0	0	0	0	0	0	0	0
<i>p</i> -value MCS	21	22	26	17	19	16	18	22	20	26	25
<i>QLIKE</i>	0.183	0.239	0.345	0.184	0.185	0.179	0.185	0.179	0.178	0.159	0.163
<i>p</i> -value <i>dm_{RV}</i>	—	2	5	1	1	7	2	5	7	25	23
<i>p</i> -value <i>dm_{SV}</i>	—	—	7	2	2	4	2	5	5	24	19
<i>p</i> -value <i>dm_{PV}</i>	—	—	—	3	3	3	3	4	3	7	6
<i>p</i> -value MCS	1	5	20	3	4	3	3	4	2	24	9

Note: The table reports the **one-step ahead** forecasting performance of the different models. The top panel shows the results for the DJIA index.

Diebold-Mariano *p*-values < 0.05 are highlighted in bold. The bottom panel reports the average loss and 5% rejection frequency of the Diebold-Mariano tests for each individual stocks. The one-sided tests between each forecasting model against RV-HAR, SV-HAR, and PV(3)-HAR are denoted by dm_{HAR} , dm_{SV} , and $dm_{PV(3)}$, respectively. MCS denotes the *p*-value of that model being in the Model Confidence Set, or the number of times that model is in the 80% Model Confidence Set. $PV(3)$ denotes the HAR-PV(3) model with 3 decompositions defined by two thresholds at 10% and 75%.

Table 11: Forecasting performance: 2015-2019 (1,258 days).

	<i>RV</i>	<i>SV</i>	<i>PV(3)</i>	<i>SV_{bu}</i>	<i>TSV_{bu}</i>	<i>PV(3)_{bu}</i>	<i>TPV(3)_{bu}</i>	<i>SV_{shr}</i>	<i>TSV_{shr}</i>	<i>PV(3)_{shr}</i>	<i>TPV(3)_{shr}</i>
<i>Panel A: DJIA index</i>											
<i>MSE</i>	3.910	4.096	4.141	3.610	3.608	3.561	3.583	3.752	3.607	3.702	3.578
<i>p</i> -value <i>dm_{RV}</i>	—	0.838	0.854	0.012	0.065	0.011	0.084	0.076	0.004	0.057	0.005
<i>p</i> -value <i>dm_{SV}</i>	—	—	0.605	0.016	0.038	0.013	0.044	0.015	0.015	0.019	0.012
<i>p</i> -value <i>dm_{PV}</i>	—	—	—	0.017	0.041	0.012	0.047	0.028	0.015	0.009	0.009
<i>p</i> -value MCS	0.485	0.464	0.192	0.498	0.723	1.000	0.919	0.404	0.671	0.424	0.615
<i>QLIKE</i>	0.245	0.236	1.482	0.220	0.222	0.214	0.219	0.220	0.214	0.221	0.214
<i>p</i> -value <i>dm_{RV}</i>	—	0.206	0.847	0.160	0.210	0.128	0.187	0.153	0.126	0.176	0.130
<i>p</i> -value <i>dm_{SV}</i>	—	—	0.847	0.133	0.220	0.090	0.184	0.120	0.090	0.158	0.095
<i>p</i> -value <i>dm_{PV}</i>	—	—	—	0.153	0.154	0.152	0.153	0.153	0.152	0.153	0.152
<i>p</i> -value MCS	0.758	0.684	0.360	0.680	0.561	0.982	0.587	0.802	1.000	0.522	0.870
<i>Panel B: Individual stocks</i>											
<i>MSE</i>	30.422	39.697	43.397	30.482	28.721	30.197	28.037	35.764	29.017	36.386	28.804
<i>p</i> -value <i>dm_{RV}</i>	—	0	0	1	1	3	1	0	2	0	5
<i>p</i> -value <i>dm_{SV}</i>	—	—	1	3	1	4	1	3	2	2	3
<i>p</i> -value <i>dm_{PV}</i>	—	—	—	1	1	1	1	2	2	2	2
<i>p</i> -value MCS	24	26	25	25	25	25	24	26	26	24	26
<i>QLIKE</i>	0.269	0.256	0.305	0.186	0.138	0.163	0.135	0.172	0.133	0.162	0.127
<i>p</i> -value <i>dm_{RV}</i>	—	0	4	2	2	3	2	1	3	10	10
<i>p</i> -value <i>dm_{SV}</i>	—	—	9	6	4	7	4	6	7	13	13
<i>p</i> -value <i>dm_{PV}</i>	—	—	—	3	4	5	4	5	5	9	8
<i>p</i> -value MCS	22	20	23	22	18	18	21	20	19	21	24

Note: The table reports the **one-step ahead** forecasting performance of the different models. The top panel shows the results for the DJIA index.

Diebold-Mariano *p*-values < 0.05 are highlighted in bold. The bottom panel reports the average loss and 5% rejection frequency of the Diebold-Mariano tests for each individual stocks. The one-sided tests between each forecasting model against RV-HAR, SV-HAR, and PV(3)-HAR are denoted by dm_{HAR} , dm_{SV} , and $dm_{PV(3)}$, respectively. MCS denotes the *p*-value of that model being in the Model Confidence Set, or the number of times that model is in the 80% Model Confidence Set. $PV(3)$ denotes the HAR-PV(3) model with 3 decompositions defined by two thresholds at 10% and 75%.

Table 12: *Forecasting performance: 2020-2022 (629 days).*

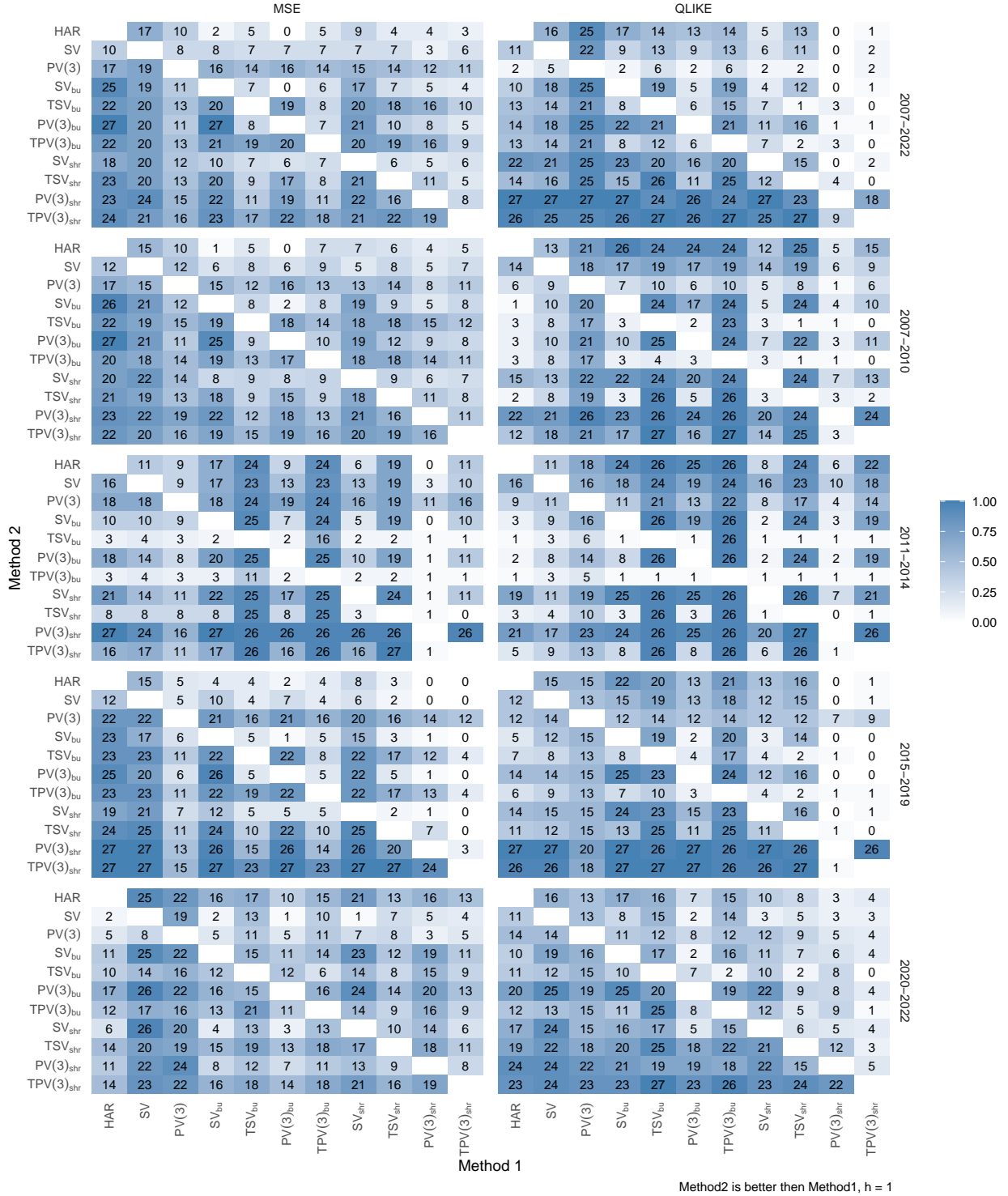


Figure 28: Qualitative evaluation of the *one-step ahead* forecasting accuracy. Each cell reports the number of times the forecasting model in the row outperforms the model in the column. Different test periods, from the top: 2007-2010, 2011-2014, 2015-2019, 2020-2022.

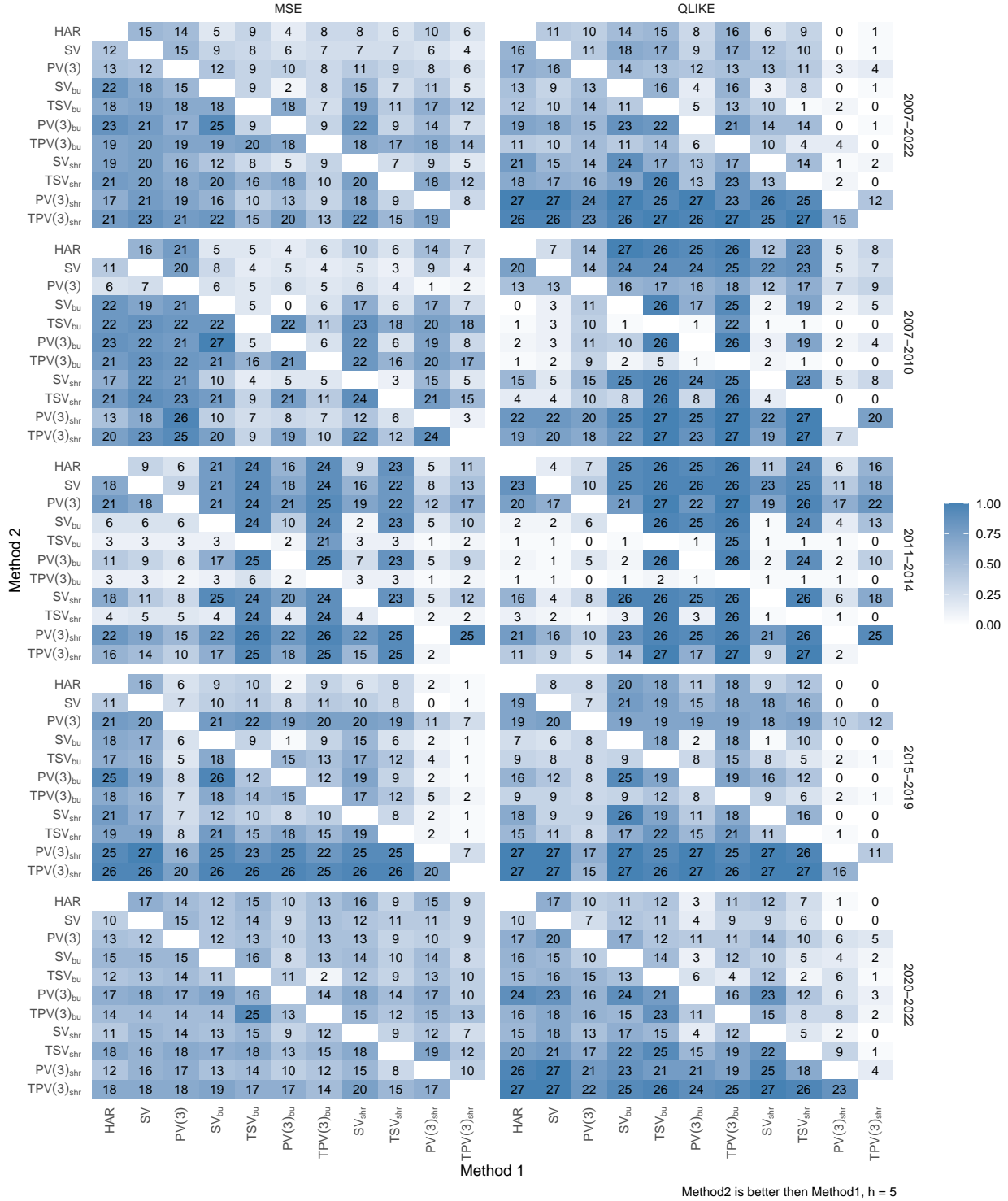


Figure 29: Qualitative evaluation of the *five-step ahead* forecasting accuracy. Each cell reports the number of times the forecasting model in the row outperforms the model in the column. Different test periods, from the top: 2007-2010, 2011-2014, 2015-2019, 2020-2022.

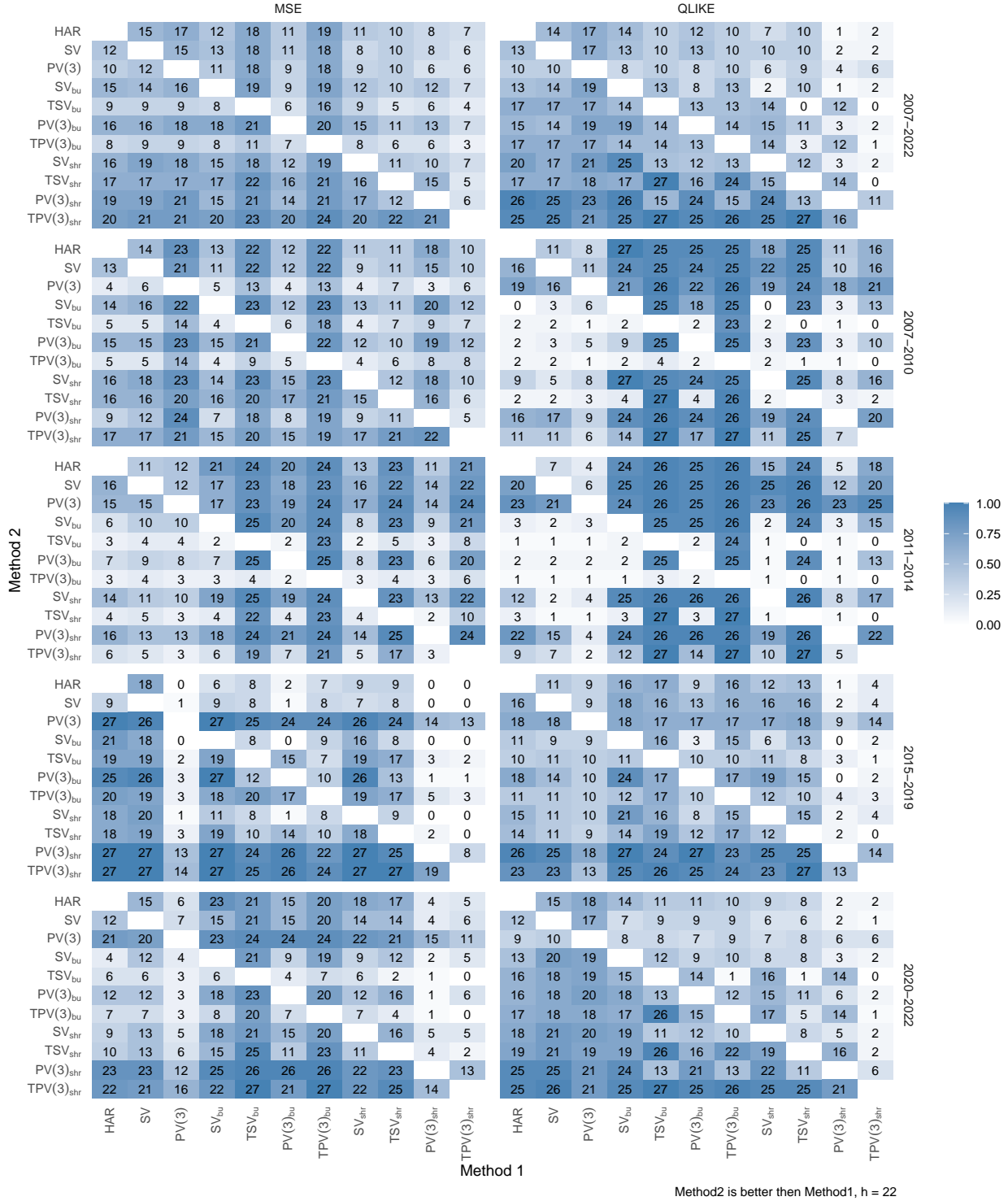


Figure 30: Qualitative evaluation of the 22-step ahead forecasting accuracy. Each cell reports the number of times the forecasting model in the row outperforms the model in the column. Different test periods, from the top: 2007-2010, 2011-2014, 2015-2019, 2020-2022.